energies

MDPI

Article

A Novel Approach to Achieve MPPT for Photovoltaic System Based SCADA

Bilal Naji Alhasnawi [1,*], Basil H. Jasim [2], Arshad Naji Alhasnawi [3], Bishoy E. Sedhom [4], Ali M. Jasim [2,5], Azam Khalili [6], Vladimír Bureš [7], Alessandro Burgio [8] and Pierluigi Siano [9,10,*]

1 Department of Computer Technical Engineering, College of Information Technology, Imam Ja'afar Al-Sadiq University, Al-Muthanna 66002, Iraq
2 Electrical Engineering Department, Basrah University, Basrah 61001, Iraq
3 Department of Biology, College of Education for Pure Sciences, Al-Muthanna University, Samawah 66001, Iraq
4 Electrical Engineering Department, Faculty of Engineering, Mansoura University, Mansoura 35516, Egypt
5 Department of Communications Engineering, Iraq University College, Basrah 61001, Iraq
6 Department of Electrical Engineering, Malayer University, Malayer 65719-95863, Iran
7 Faculty of Informatics and Management, University of Hradec Králové, 50003 Hradec Králové, Czech Republic
8 Independent Researcher, 20124 Milano, Italy
9 Management and Innovation Systems Department, Salerno University, 84084 Fisciano, Italy
10 Department of Electrical and Electronic Engineering Science, University of Johannesburg, Johannesburg 2006, South Africa
* Correspondence: bilalnaji11@yahoo.com (B.N.A.); psiano@unisa.it (P.S.)

Abstract: In this study, an improved artificial intelligence algorithms augmented Internet of Things (IoT)-based maximum power point tracking (MPPT) for photovoltaic (PV) system has been proposed. This will facilitate preventive maintenance, fault detection, and historical analysis of the plant in addition to real-time monitoring. Further, the simulation results validate the improved performance of the suggested method. To demonstrate the superiority of the proposed MPPT algorithm over current methods, such as cuckoo search algorithms and the incremental conductance approach, a performance comparison is offered. The outcomes demonstrate the suggested algorithm's capability to track the Global Maximum Power Point (GMPP) with quicker convergence and less power oscillations than before. The results clearly show that the artificial intelligence algorithm-based MPPT is capable of tracking the GMPP with an average efficiency of 88%, and an average tracking time of 0.029 s, proving both its viability and effectiveness.

Keywords: MPPT; SCADA; solar system; Internet of Things

check for updates

Citation: Alhasnawi, B.N.; Jasim, B.H.; Alhasnawi, A.N.; Sedhom, B.E.; Jasim, A.M.; Khalili, A.; Bureš, V.; Burgio, A.; Siano, P. A Novel Approach to Achieve MPPT for Photovoltaic System Based SCADA. *Energies* **2022**, *15*, 8480. https://doi.org/10.3390/en15228480

Academic Editor: Manolis Souliotis

Received: 12 October 2022
Accepted: 9 November 2022
Published: 13 November 2022

1. Introduction

The world has started to move away from fossil fuels (coal, petroleum, and natural gas) in the last few decades for a variety of reasons. Some nations use renewable energy sources because there are insufficient fossil fuel reserves left; some nations have switched to renewable energy sources because they never had fossil fuel reserves and must import from oil-producing nations, which has an impact on their annual budget; and some nations have switched to renewable energy sources because they are pollution- and noise-free. This indicates that in order to meet their energy needs without hurting the environment, all nations are turning to renewable energy sources. Almost 25% of all electricity in 2019 came from renewable sources, and that percentage is undoubtedly higher now.

The most widely used renewable energy source is solar because of its simple installation, low maintenance requirements, and environmental friendliness [1]. Long regarded as a clean and green energy source, solar photovoltaic (PV) power generation offers several benefits, including being environmentally benign, silent, and requiring minimal maintenance. However, because the PV characteristics are nonlinear, operating at the maximum power point (MPP) to create the most output power is a difficult problem. As a result, when solar insolation and cell temperature change, solar PV panel properties including current (I)-voltage (V) and power (P)-voltage (V) characteristics are affected. Consequently, it is crucial to monitor the MPP using the PV panel's profile. Using MPPT techniques, the maximum output power from the PV module is harvested, and a power electronic-based converter is crucial to this process. As a result, the MPP can be monitored by modifying the power electronics converter's duty cycle. The literature considers a number of converter types, including boost, buck, buck-boost, interleaved converter, and SEPIC converters. The MPPT controller is offered with each PV system as a necessary component [2].

The Internet of Things (IoT) is an intriguing concept that explains the interactions between intelligent agents and gadgets via Internet Protocol (IP) networks. It is defined by contemporary communication techniques. IoT enables the tracking, sensing, and organization of environmental states for numerous sensors, including intelligent transportation, intelligent healthcare, home automation, and smart communities [3].

IoT-based technologies enable dispersed connectivity and automation for the MPPT system, which processes sensor data and supplies it to the antenna to be controlled and monitored. Additionally, IoT makes it possible to dynamically locate a solar module's MPP zone. The generation, transmission, and distribution of PV power systems across the operation are all made possible by the Internet of Things (IoT), which offers the connectivity and automation required for MPPT operations. It has smart meters, sensors, and actuators that allow the PV power system to perform MPPT operations [4–8].

Many researchers have developed a variety of methods to improve the tracking precision and productivity of solar power-producing systems. Table 1 lists the benefits and drawbacks of several MPPT approaches.

Table 1. Summary of the benefits and drawbacks of some MPPT approaches.

Ref.	Achievements	Advantages	Limitations
[9]	1. Introducing a remote monitoring system for solar power plants.	1. High tracking efficiency, and few parameters require tuning.	1. Large search space, computational complexity, high cost, and hardware implementation. 2. The IoT layer platform's data processing and storage are not taken into account.
[10]	1. Presenting a novel artificial intelligence MPPT technique for Integrated PV-WT-FC Frameworks.	1. Easy to implement, simple structure, and low cost.	1. The IoT layer platform's data processing and storage are not taken into account. 2. Steady-state oscillation, no guarantee for convergence, drift problem, reduced efficiency, and frequent tuning of specific parameters.
[11]	1. Performing a prototype for the online monitoring of PV-MPPT using IoT technology.	1. Higher tracking accuracy reduced power oscillation, and tracking efficiency is higher than 87%.	1. High cost, difficult to control, steep in hardware implementation, and convergence is assured if the global peak is situated outside the search zone.
[12]	1. Introducing a new construction of a maximum power point tracker (MPPT) for partially shaded PV panels using a Raspberry Pi 4-based embedded board programmed via two approaches cuckoo search (CS) and particle swarm optimizer (PSO).	1. Fast convergence and tracks true MPPT during partial shading conditions. 2. High efficiency.	1. Large search space, computational complexity, high cost, and hardware implementation.

Table 1. *Cont.*

Ref.	Achievements	Advantages	Limitations
[13]	1. Introducing a real-time data acquisition of photovoltaic panel parameters via IoT.	1. It is advantageous compared to other swarm-based optimization strategies because of its strong properties.	1. The energy conversion efficiency of a PV system is not greater than 16% or 17%, especially when the irradiation level is below standard test condition (STC), and the power generated by the PV system continuously varies with the climatic condition.
[14]	1. Introducing an IoT-based smart solar energy monitoring system.	1. The primary goal of this work is to investigate how the MPPT method extracts the most power possible from photovoltaic modules under various sun radiation and temperature conditions.	1. High cost, difficult to control, steep in hardware implementation, and convergence is assured if the global peak is situated outside the search zone.
[15]	1. Presenting IoT-based sustainable wind green energy for smart cites using fuzzy logic.	1. Higher tracking accuracy reduced power oscillation.	1. Steady-state oscillation, no guarantee for convergence, drift problem, reduced efficiency, and frequent tuning of specific parameters.
[16]	1. Introducing a new optimization algorithm-based MPPT control technique for PV systems.	1. Higher tracking accuracy reduced power oscillation.	1. It is outside the purview of this work to conduct an extensive analysis on a particular application's buck, boost, or buck-boost dc-dc converter.
[17]	1. Implementing MPPT using modified butterfly optimization algorithm.	1. Possesses a simple and cost-effective technique for practical implementation 2. Good convergence speed and efficient for partially shaded conditions.	1. An uninvestigated cloud-based platform for MPPT systems in smart grid.
[18]	1. Enhancing global maximum power point of photovoltaic using chimp optimization algorithm.	1. Simple structure. 2. Easy to implement.	1. A lot depends on the converter utilized, and a change in the converter will necessitate considerable changes to the controller.
[19]	1. Proposing a novel global MPPT method for PV systems based on the squirrel search algorithm.	1. Fast convergence. 2. Have fewer control parameters.	1. Not looked at for IoT systems that rely on GMPP tracking.
[20]	1. Introducing global hybrid maximum power point tracking for PV modules based on a double-diode model.	1. Facilitating the increase or decrease of the duty ratio.	1. Not looked at for IoT systems that rely on GMPP tracking.
[21]	1. Presenting global maximum power point tracking of photovoltaic module arrays based on bee colony algorithm.	1. Robust and simple design. 2. High efficiency.	1. These methods incur extra hardware and cost.

Table 1. *Cont.*

Ref.	Achievements	Advantages	Limitations
[22]	1. Design and creation of a low-cost, mobile, on-field I-V curve tracer based on capacitor loading for solar photovoltaic modules with high power ratings.	1. Designed according to changes in power and voltage based on P-V curve to offer a very direct approach.	1. Such artificial intelligence techniques call for lengthy computations in addition to their intricate hardware implementation.
[23]	1. Presenting an adaptive robust fuzzy PI controller for MPPT of PV system.	1. Easy to implement, simple structure, and low cost.	1. This system possesses steady-state errors and is system-dependent.
[24]	1. Introducing an improved particle swarm optimization-based MPPT for PV system operating.	1. High tracking efficiency, and few parameters require tuning.	1. Earlier heuristic approaches had slow dynamic behavior, necessitating a lot of iterations (MPPT steps) to follow the GMPP.
[25]	1. Introducing a PSO-based MPPT algorithm for PV systems operating.	1. Higher tracking accuracy reduced power oscillation.	1. These techniques are only appropriate for systems with several converters.
[26]	1. Presenting application of modified PSO for MPPT.	1. High efficiency. 2. Robust and simple design.	1. To track MPP, these hill-climbing techniques actively induce perturbations.
[27]	1. Introducing an improved particle PSO-based MPPT strategy.	1. Fast convergence. 2. High tracking efficiency, and few parameters requires tuning.	1. The IoT layer platform's data processing and storage are not taken into account.
[28]	1. MATLAB/Simulink model development for a battery energy storage system.	1. High efficiency.	1. Not looked at for IoT systems based on GMPP tracking.
[29]	1. Presenting the circuitry modeling of the standalone MATLAB/Simulink environment solar photovoltaic MPPT lead-acid battery charge controller.	1. Higher tracking accuracy.	1. The IoT layer platform's data processing and storage are not taken into account.

The following is a summary of this paper's significant contributions:

1. To address the aforementioned disadvantages, a controller for MPPT is used in this study. The controller tracks the maximum power point (MPP) in real-time.
2. To prevent failure in tracking the MPP under a rapid change in solar insolation, the authors of this study suggest an easy and precise MPPT technique. By considering the change in output current profile in addition to the conventional MPPT technique, the divergence problem and the steady-state power oscillation are diminished. Both fixed step sizes and variable step sizes are used to test the suggested modified ABC approach. Between the load and photovoltaic module, a dc-dc converter is necessary to implement this method. In order to achieve the MPPT's goals, the classic boost converter is chosen and efficiently developed in this article based on system ratings.
3. The goal of this effort is to create and implement a low-cost prototype for online monitoring of a PV system's maximum power output. The prototype also includes a web portal that enables customers to view changes in the amount of power being generated by their installations in real time without exerting more effort or spending extra money. Verifying the effectiveness of some current MPPT algorithms using IoT technology in real time is another goal.
4. Comparison to incremental conductance method, cuckoo search algorithm and an improved Artificial Bee Colony (ABC) algorithm is conducted.

2. Problem Formulation

The solar generator's output must be extracted by the MPPT arrangement, as shown Figure 1. It consists of the load, the MPPT instruction, the converter, and the PVG. PVG transforms solar energy into a storable direct electric current. Converters for DC to DC are choppers. Due to the MPPT command, which creates and modifies a suitable Pulse Width Modulation (PWM) signal, their function is used to automatically match the load to the PVG. The PVG consists of one or more solar panels that are connected to increase the current and voltage produced by the entire system. Numerous solar cells are arranged in series and parallel on the solar panel [30,31].

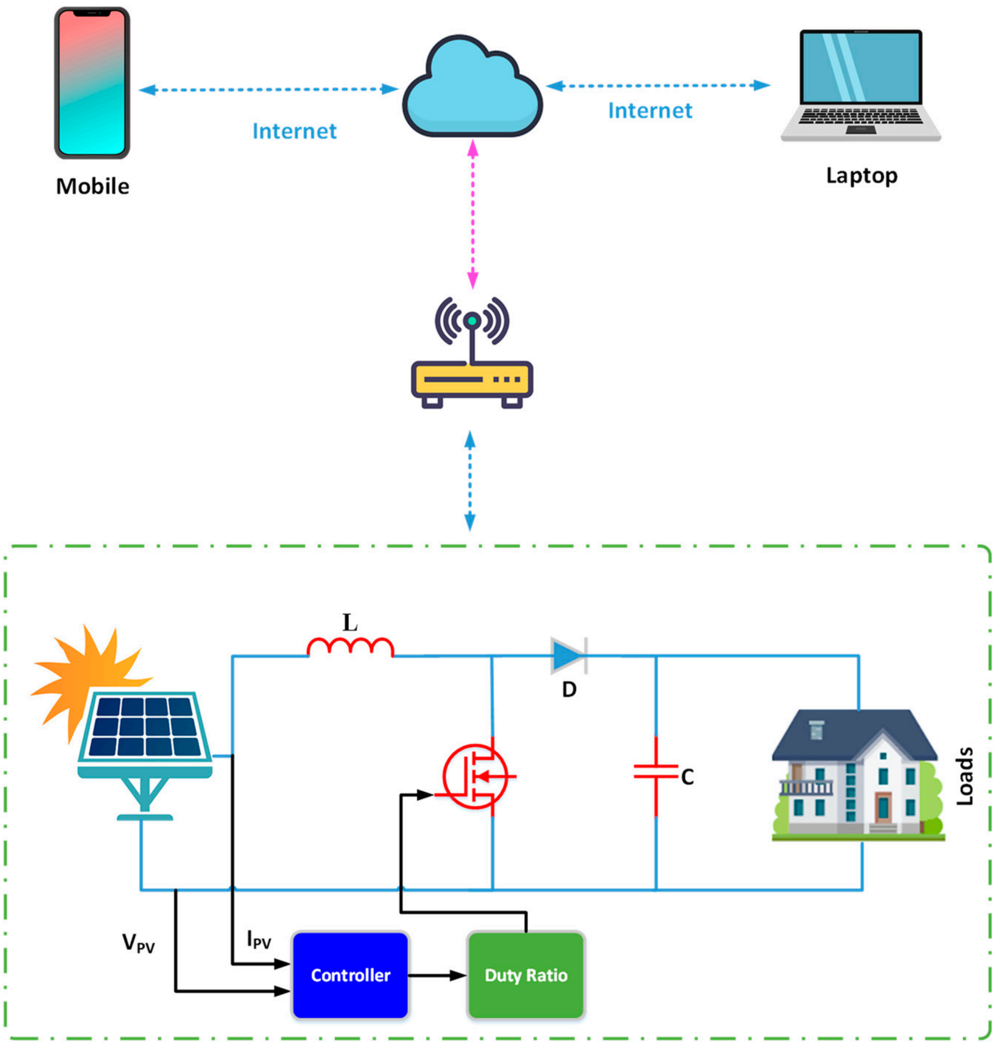

Figure 1. Structure of proposed system.

The converter can fix an issue via altering a duty ratio, since the operating point of the photovoltaic panel is mostly determined via impedance mismatch between loads and photovoltaic. Figure 1 depicts the block diagram of the entire PV system.

As previously mentioned, the switch's duty cycle has been modified for MPPT control. The duty cycle regulation, however, can be justified in light of converter efficiency. The relationship between output and input can be used to calculate the efficiency of conventional converter ($\eta_{\text{Converter}}$), and the relationship is shown in the equations below [2].

$$\eta_{\text{Converter}} = \left(\frac{1}{1-D}\right)^2 \frac{R_{\text{in}}}{R_0} \quad (1)$$

where R_{in} is the input resistance and R_0 denote photovoltaic output resistance, respectively; input resistance can be represented as:

$$R_{in} = \eta_{Converter} \times (1 - D)^2 \times R_0 \quad (2)$$

Equation (3) shows that the converter duty cycle can be changed to control the operating point. The operating point variation, with respect to the load line, is shown in Figure 2. Slope variation and steady-state performance are shown in Figure 3.

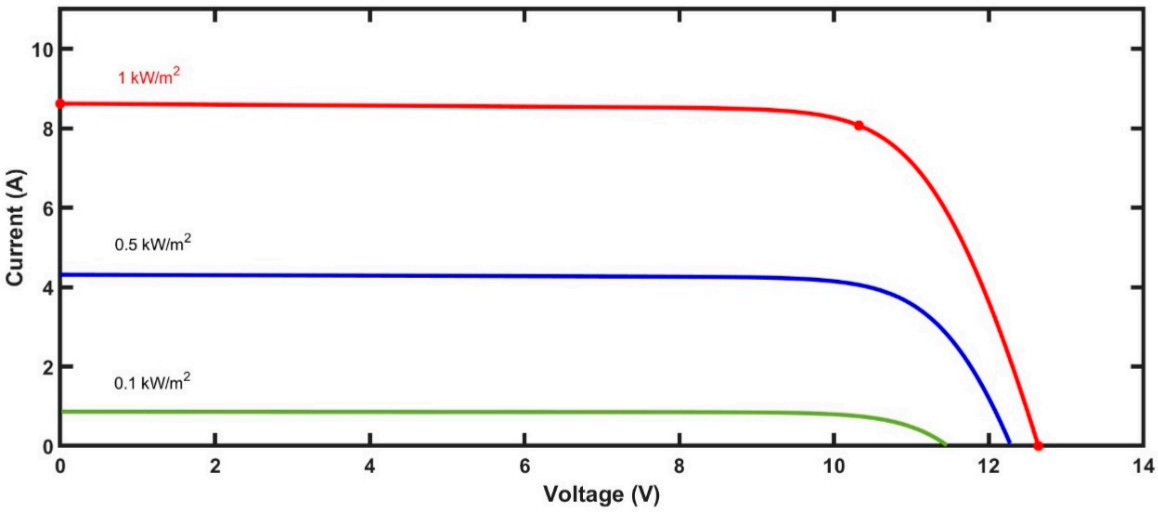

Figure 2. Variation in operating points with respect to the load line.

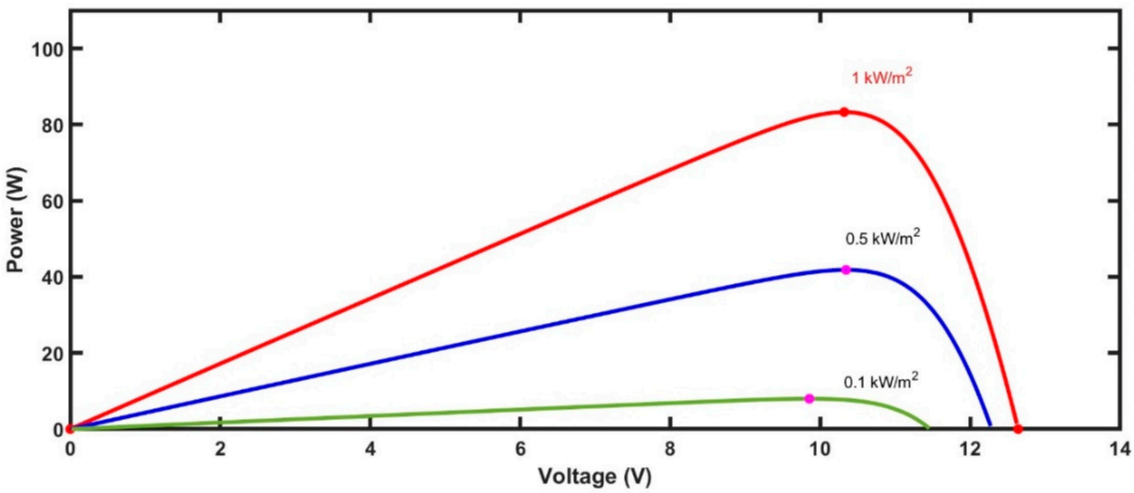

Figure 3. Slope variation and steady-state performance.

IoT is the extensive system of knowledge objects connected to the internet, which can identify and communicate data on the internet to objects. This work uses IoT to provide a web server for WiFi clients. The proposed system is shown in Figure 1.

The Thing Speak framework and MATLAB program exchange data in real time to represent the suggested communication structures. Because of the following benefits, ThingSpeak has been used to simulate real-time communication in cloud-based approaches [31]:

1. It enables two-way communication between the user and the simulated system, enabling real-time data sharing and remote control.
2. A platform for communication that enables online real-time data sharing between MATLAB and ThingSpeak.

3. Security—each channel has its own ID and can be either public (visible by other users) or private. User authentication is enabled via username and password (seen by specific users).

Modeling of Photovoltaic

The installed maximum power and weather conditions affect how much power the PV panels can produce. The photovoltaic output power depends on irradiance, the efficiency of generation, the area of the panels, and the optimal orientation depending on the location. The chosen PV technology has an efficiency η_{PV} = 15%. The power produced by PV over a day is given as follows [32–34]:

$$I = I_{ph;cell} - I_{0;cell}\left[\exp\left(\frac{q(V + IR_{s;cell})}{akT}\right) - 1\right] - \frac{V + IR_{s;cell}}{R_{p;cell}} \tag{3}$$

where I_{PH}, is the cell photocurrent (A), I_0 is the saturation current of photovoltaic, Id is the current computed by Shockley diode equation, q is the electron charge (1.602×10^{-19} C), T is the temperature of the diode measured in Kelvin (K), k is the Boltzmann's constant (1.38×10^{-23} J/K), R_p is the cell parallel resistance of PV cell (Ω), R_s is the cell series resistance of PV cell (Ω). Figure 4 shows the PV cell's equivalent circuit [35].

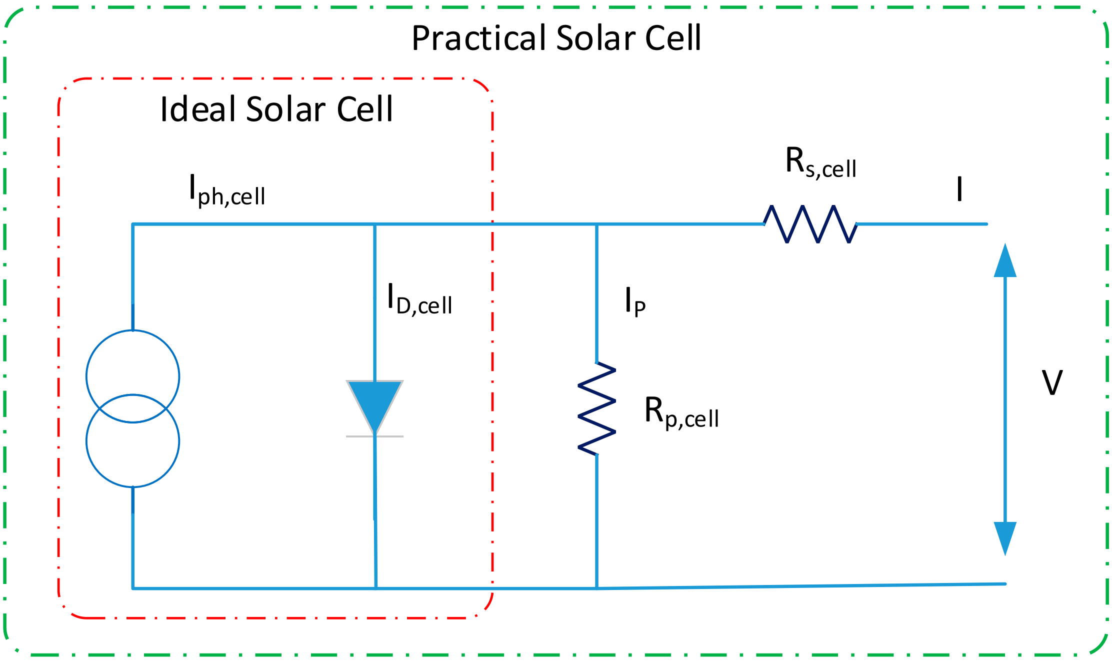

Figure 4. The PV cell's equivalent circuit [35].

The I–V curve for the perfect PV cell, derived from the aforementioned equation, is shown in Figure 5. It should be remembered that the difference between the PV cell's I_{PH}, cell and I_d cell produces output cell current (I) [35].

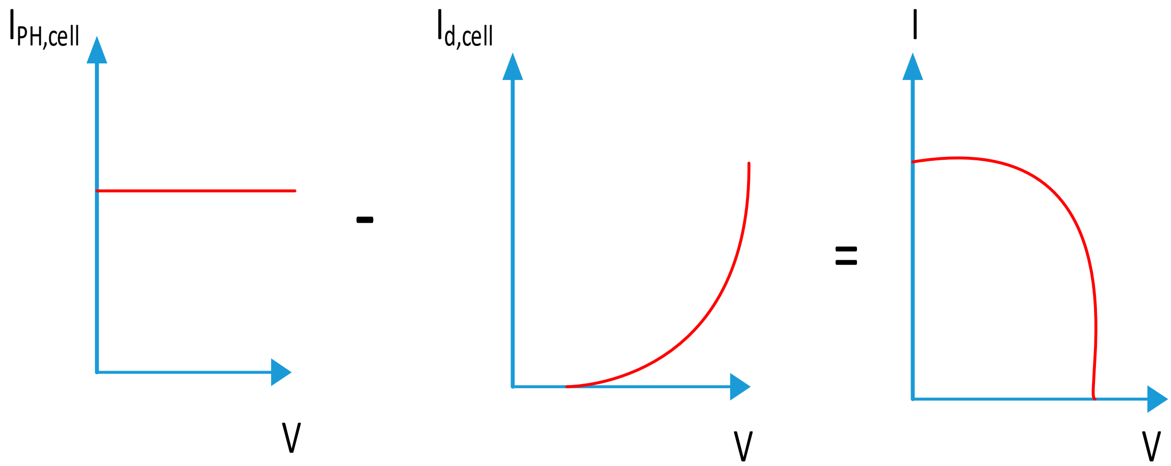

Figure 5. A typical current and voltage curve of photovoltaic.

Photovoltaic Modeling

As previously mentioned, a photovoltaic module is made up of solar cells connected in parallel and in series. Equation (4) is used to obtain the fundamental mathematical equation, and the voltage and current characteristics of the photovoltaic module are described as follows [36]:

$$I = I_{ph,cell} - I_0\left[\exp\left(\frac{V + IR_S}{a\,Vt}\right) - 1\right] - \frac{V + IR_S}{R_p} \quad (4)$$

where $I_{ph,\,cell}$ is photocurrent (A), V_t is photovoltaic thermal voltage, I_0 is PV reverse leakage current, R_s is PV series resistance, R_p is parallel resistance. The current and voltage curves seen in Figure 6 are produced by Equation (4).

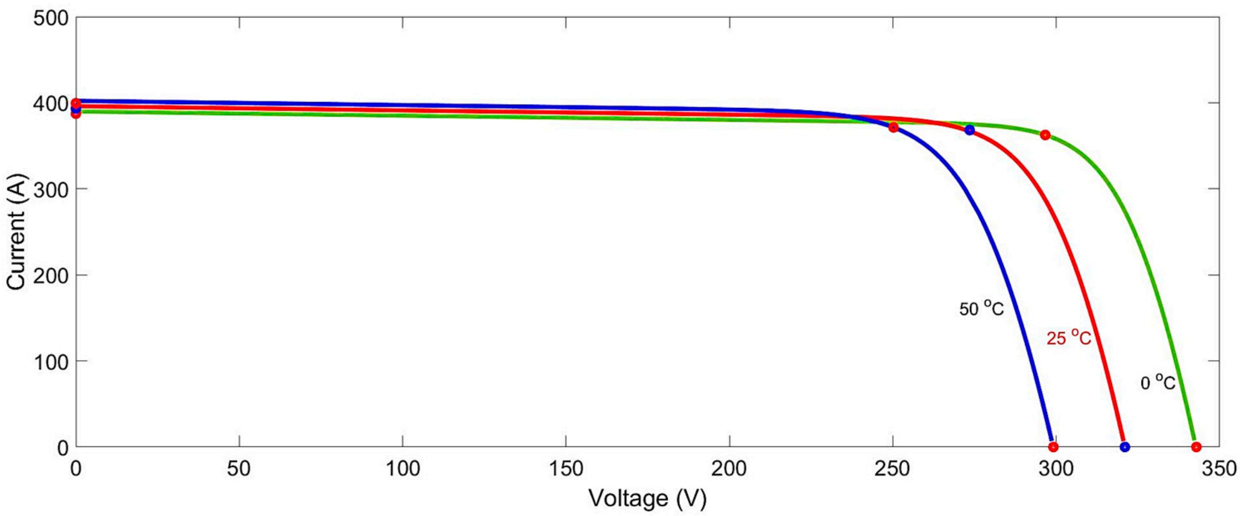

Figure 6. A typical photovoltaic current-voltage curve.

The amount of PV irradiance hitting the module and the temperature of the photovoltaic cell both affect the photocurrent for a photovoltaic (I_{ph}). This is equivalent to Equation (5):

$$I_{ph} = \frac{G}{G_n}\left(I_{ph;n} + K_i\Delta T\right) \quad (5)$$

where ΔT is the difference in degrees Celsius between the photovoltaic cell's actual temperature (T) and its nominal temperature (T_n), K_i is temperature coefficient, G_n is nominal irradiance (1000 w/m^2), G is the measured PV irradiance in w/m^2, $I_{ph;n}$ denotes the photocurrent. The voltage of the open circuit (V_{oc}) is affected by the cell temperature as [37,38]:

$$V_{oc} = V_{oc;n} + K_v \Delta T \tag{6}$$

where K_v is the voltage of the open circuit temperature coefficient, $V_{oc;n}$ is the voltage of the open circuit under nominal conditions. To determine the diode saturation current (I_0), apply the equation below:

$$I_0 = \frac{I_{sc;n} + K_i \Delta T}{\exp\left(\frac{V_{oc;n} + K_v \Delta T}{a\ V_t}\right) - 1} \tag{7}$$

where $I_{sc;n}$ represents the short circuit current under ideal circumstances.

3. MPPT Based on the IC Approach

The incremental conductance method is the MPPT that is most frequently employed for PV systems. The observation that a PV module's power derivative with respect to voltage is positive to the left of the MPP, zero at the MPP, and negative to the right of the MPP serves as the basis for the theory [39,40]:

$$\begin{cases} \frac{dP}{dV} > 0 & \text{left of MPP} \\ \frac{dP}{dV} = 0 & \text{at PP} \\ \frac{dP}{dV} < 0 & \text{right PP} \end{cases} \tag{8}$$

where:

$$\frac{dP}{dV} = \frac{d(VI)}{dV} = I + V\frac{dI}{dV} \cong I + V\frac{\Delta I}{\Delta V} \tag{9}$$

Equation (9) can be modified as:

$$\begin{cases} \frac{\Delta I}{\Delta V} > -\frac{I}{V} & \text{left of MPP} \\ \frac{\Delta I}{\Delta V} = -\frac{I}{V} & \text{at MPP} \\ \frac{\Delta I}{\Delta V} < -\frac{I}{V} & \text{right MPP} \end{cases} \tag{10}$$

Thus, as illustrated in the flow chart in Figure 7, the MPP can be monitored via comparing instantaneous conductance $\left(\frac{I}{V}\right)$ to IC ($\frac{\Delta I}{\Delta V}$). As a result, the quantity $\left(\frac{\Delta I}{\Delta V}\right) + \left(\frac{I}{V}\right)$ has a sign that denotes the right perturbation's direction leading to the MPPT. When the MPP is reached, the photovoltaic continues to operate at this time and a perturbation is terminated unless a change in ΔI is noticed. To keep track of the new MPP in this situation, the program either decreases or increases the V_{ref}. The perturbation step size (ΔD) controls the tracking speed of the MPP. The trade-off between a fast dynamic reaction and steady state performance makes choosing the perturbation step size challenging. It is important to understand that the constant voltage methodology outperforms the IC method when the PV module is exposed to low amounts of radiation, since the perturbation may be terminated because the change in ΔI is too small.

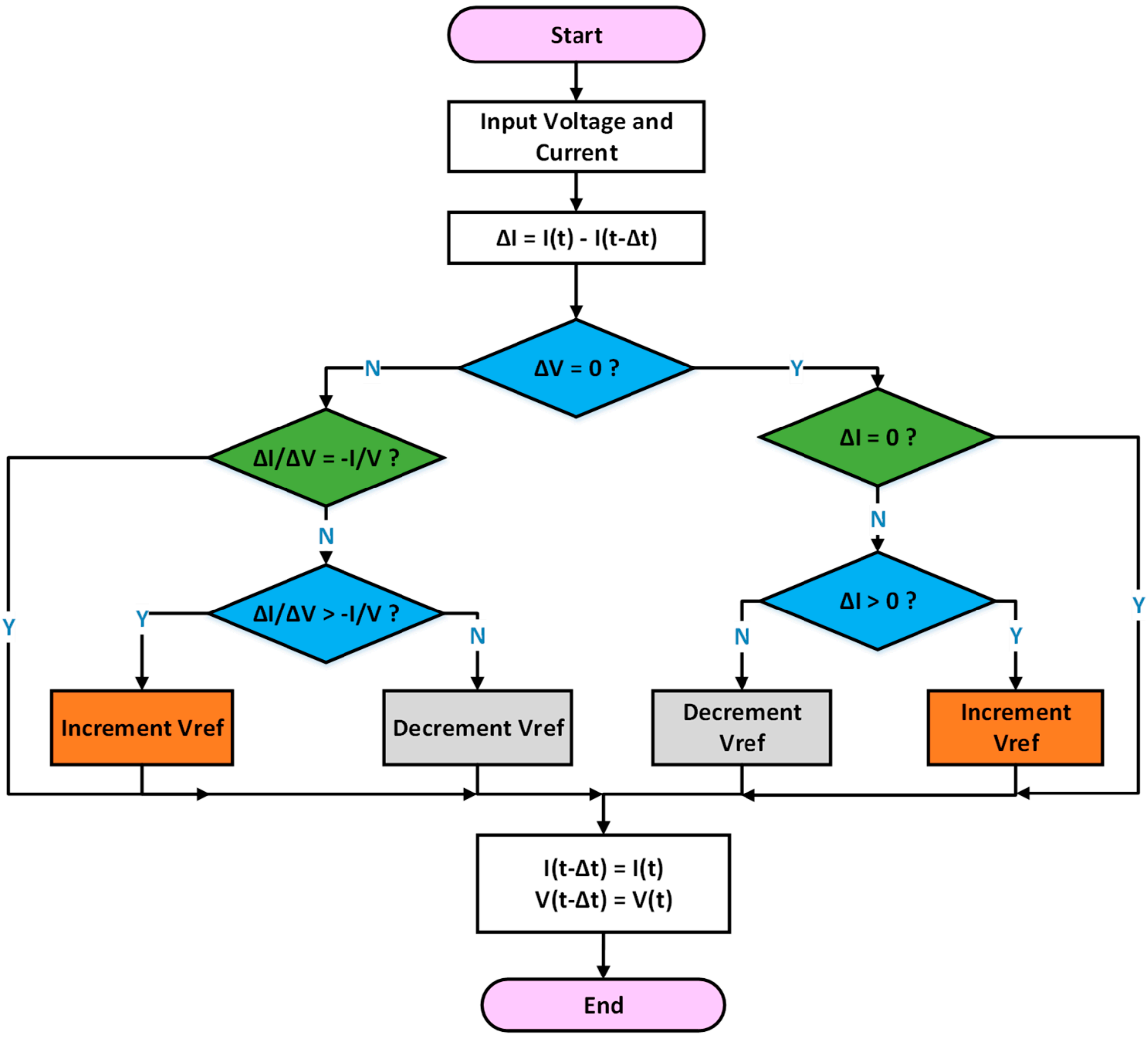

Figure 7. MPPT based on an incremental conductance flow chart [39].

4. Application of Cuckoo Search Algorithm toward MPPT

The Cuckoo Search Algorithm (CSA) was first introduced in 2009 by Suash Deb and Xin-She Yang [41] and was motivated by the cuckoo bird's reproductive behavior. The eggs of cuckoo birds are laid in host nests, allowing them to hatch sooner. The young cuckoo birds break some of the host bird's eggs in order to maximize their chances of surviving by hoarding all the food. In most cases, the host birds kill the eggs or quit the nest when they learn that the eggs in their nests are alien eggs. Therefore, cuckoo birds adopt a novel strategy by laying more eggs in more than one nest in order to maximize the viability of their eggs [42].

4.1. *Lévy Flight*

Small, medium, and big step sizes are randomly used while looking for a host nest among several host nests. The Lévy flying random mathematical function is shown to theoretically mirror the fluctuations in step sizes during host nest hunting. In other words, the power law distribution shown below is used to calculate the random step sizes of the Cuckoo search method using the Lévy flight random mathematical function [42]:

$$y = l^{-\lambda} \quad (11)$$

where l is flight length and λ is a variance. The Lévy flight model produces a distribution of search steps. This method has shown its efficacy in situations including multimodal, multiple objectives, and nonlinear optimization. The new generation of particles $x^{(t+1)}$ via cuckoo search Lévy flight is achieved by:

$$x_i^{(t+1)} = x_j^t + \alpha \oplus \text{Levy}(\lambda), \tag{12}$$

where i is a sample number, t is the iteration number, and α represents the step size $\alpha > 0$ [42].

$$\alpha = \alpha_0 \left(x_j^t + x_i^t \right), \tag{13}$$

where α_0 is the initial step.

4.2. MPPT Using CSA

It is necessary to select the right variables for the search in order to use cuckoo search for designing the MPPT. The samples, in this case defined as the PV voltage values, come first, i.e., V_i $(i = 1, 2, \ldots, n)$; where n is the total number of samples and α is step size. The fitness function (J) is a value of photovoltaic power at the MPPT. As J is dependent on the photovoltaic voltage, $J = f(V)$ [43].

Power is specified as an initial fitness value and generated samples are applied to photovoltaic modules first. The greatest power produced by its matching voltage is regarded as the best example. After performing the Lévy flight, fresh voltage samples are created using the following equation:

$$V_i^{(t+1)} = V_i^t + \alpha \oplus \text{Lvy}(\lambda). \tag{14}$$

where $\alpha = \alpha_0(v_{best} - v_i)$. In [43], a condensed version of the Lévy distribution is provided as:

$$s = \alpha_0(v_{\text{best}} - v_i) \oplus \text{Lvy}(\lambda) \approx \kappa \times \left(\frac{u}{(|v|)^{\frac{1}{f}}} \right) (v_{\text{best}} - v_i) \tag{15}$$

where u and v are determined from the normal distribution curves, $\beta = 1.5$, k is the Lévy multiplying coefficient.

$$u \approx N\left(0, \sigma_u^2\right) v \approx N\left(0, \sigma_v^2\right) \tag{16}$$

If Γ is integral gamma function, variable σ_u and σ_v are represented by:

$$\sigma_u = \left(\frac{\Gamma(1+\beta) \times \sin(\pi \times \beta/2)}{\Gamma\left(\left(\frac{1+\beta}{2}\right)\right) \times \beta \times (2)^{\left(\frac{\beta-1}{2}\right)}} \right)^{\frac{1}{\beta}} \text{ and } \sigma_v = 1 \tag{17}$$

The PV modules are used to measure the respective power for the new voltage samples. By contrasting the power levels, the voltage that produces the maximum power is picked as the new best sample. Other samples are also randomly destroyed with a probability of P_a in addition to this best sample; this approach simulates the discovery and subsequent destruction of the cuckoo's eggs by a host bird. The destroyed samples are then replaced with fresh ones, created at random. As a result, the powers for all samples are measured once more, and the optimal power is chosen by assessing J. Until all samples have achieved the MPP, iteration continues. Figure 8 shows the cuckoo search algorithm flowchart [43].

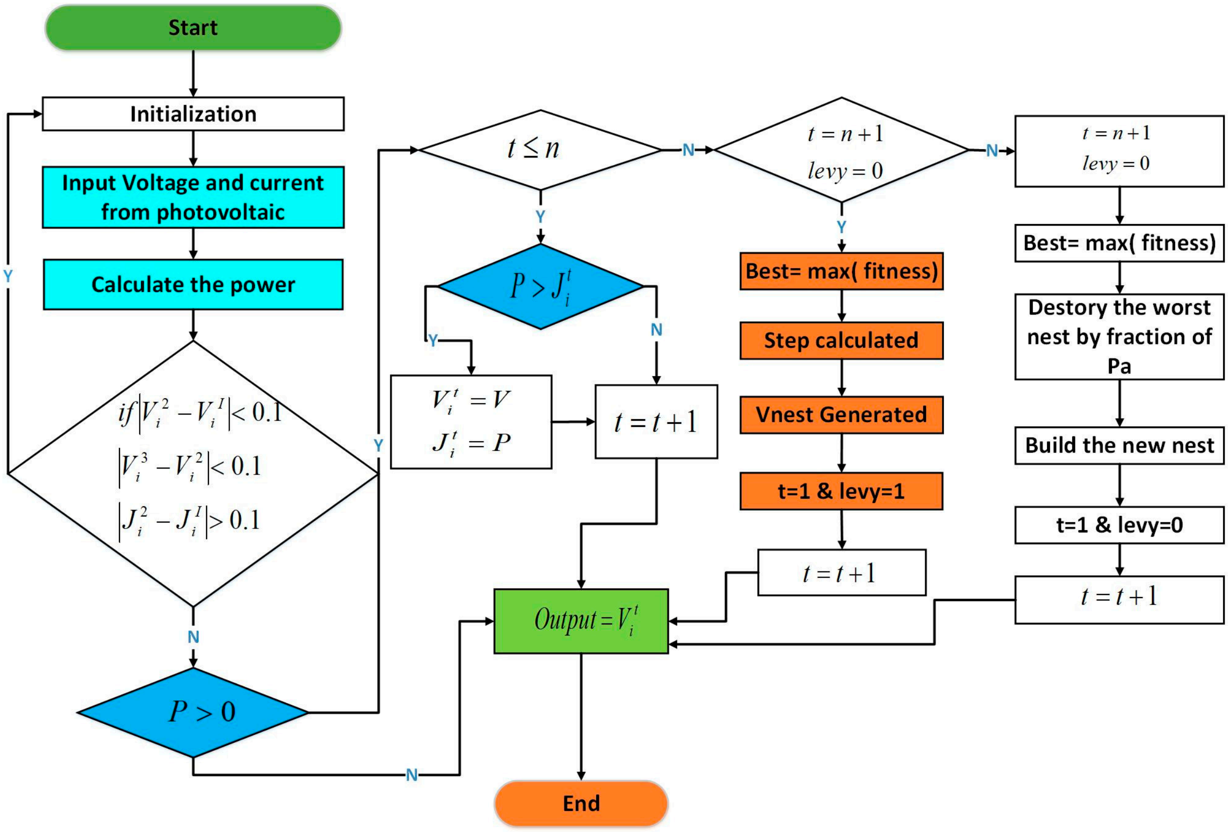

Figure 8. Cuckoo search algorithm flowchart.

5. ABC Algorithm Application to MPPT

The ABC algorithm mimics the foraging behaviors of bee colonies, and from this arises collective intelligence for boosting nectar levels in the hive. The ABC algorithm sees a food source's nectar content as the quality (fitness) of the corresponding solution, and the position of a nectar supply as a potential solution vector for a problem. Worker bees, observation bees, and scout bees are three different types of functional groups found in a genuine bee colony. A colony is made up of observers and workers. An employed bee always returns to a known nectar supply rather than choosing a new food source based only on visual cues from its surroundings. The bee recalls the new site and forgets the old one if there is more nectar at the new location than at the previous one. Bees observed at a hive migrate in the direction of the hired bee's present location of finest food supply. When the hiring process becomes unproductive, the employed bee turns into a scout and begins looking for a new position [44].

A boost-type dc-dc converter is connected for MPPT between the photovoltaic power producing system and the load. The duty ratio d of the dc-dc converter, also known as the position of the food source, acts as the decision variable in the ABC approach. The nectar quantity is thought of as the PV system's output power. By removing a scout bee phase from the ABC algorithm in this study, the GMPP convergence time is made faster. The following are the sequential steps for tracking GMPP using ABC [44].

(1) Initialization: In this piece, the employed bees are represented by one half of the colony, and the observers are represented by the other half. Using the following equation, all of these bees are initially placed in various food-source positions (i.e., duty ratio of the dc-dc converter) in a solution space.

$$x_i = d_{min} + \frac{(i-1)[d_{max} - d_{min}]}{N_p - 1} \quad (18)$$

where $i = 1, 2, \ldots, N_p$ and d_{min} and d_{max} denote minimum and maximum values of a duty-ratio.

(2) Evaluating the quantity of nectar: The simulation study's mathematical model is used to calculate output power in relation to each duty-ratio (food position). Bees are classified as employed workers or observers, depending on the amount of nectar.

(3) Locating a new food source: Each cycle of the tracking MPPT of the photovoltaic system is carried out in two parts.

(a) Employed bee phase: Each worker bee updates its location inside its neighborhood using the formula below:

$$x_{i(k+1)} = x_{i(k)} + \phi\left(x_{i(k)} - x_{j(k)}\right) \tag{19}$$

where k denotes number of iterations, variable ϕ is a random number generated between $[-1, 1]$, $j \in \{1, 2, \ldots, NP/2\}$ is a randomly chosen index where $j \neq i$.

(b) Onlooker phase: Waiting for observer bees in the dance area to come closer to the employed bee's position where there is the most nectar available. This motion is described as:

$$x_{i(k+1)} = x_{h(k)} + \frac{\phi * (d_{max} - d_{min})}{\frac{N_p}{2} - 1} \tag{20}$$

where x_h denotes food source position.

(4) Termination criterion: If, after five iterative rounds, the PV system detected by the bees does not produce any more power, end the algorithm and run a dc-dc converter at a best duty ratio.

(5) Reinitiating the search: Restart the procedure if the change in power output indicates that the solar insolation has changed.

The proposed system samples and senses the photovoltaic output power every 0.1 s, and the MPPT controller uses the following equation to determine PV output power has changed [44]:

$$\left|\frac{P_{\text{pv}}^k - P_{\text{pv}}^k}{P_{\text{pv}}^k}\right| \geq 0.1 * A_w \tag{21}$$

where A_w, or adaption weight, accounts for quickly changing environmental conditions. This variable must be carefully selected based on the region and the local climate.

If Equation (21) is accurate, it must be determined whether the change in output power is the result of a change in the load resistance or a change in the shadow pattern. The conditions listed below have been confirmed:

$$\left|\frac{V_{\text{pv}}^k - V_{\text{pv}}^{k-1}}{V_{\text{pv}}^k}\right| \geq 0.2 \tag{22}$$

$$\left|\frac{I_{\text{pv}}^k - I_{\text{pv}}^{k-1}}{I_{\text{pv}}^k}\right| \geq 0.1 \tag{23}$$

If the aforementioned conditions are verified to be true, a change in output power is caused via a change in the shade pattern; proceed to step 2 as a result. Otherwise, a small duty ratio modification will be adequate to account for the fluctuation in load resistance that is causing the change in output power. Equation (13) can be used to achieve this duty ratio modification. Figure 9 shows the proposed ABC algorithm's flowchart for easier understanding.

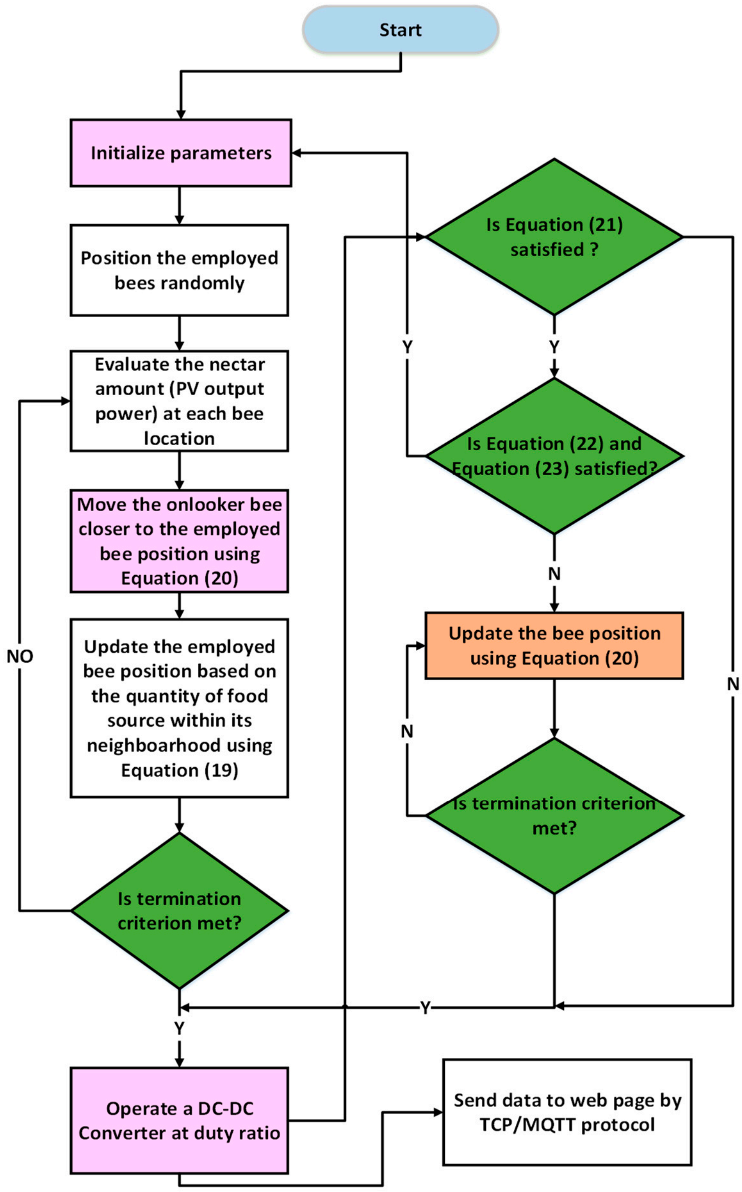

Figure 9. Flowchart of proposed algorithm.

6. Proposed Communication Platform

If there is a disruption, a smart MG's decentralized controller aids in controlling the working circumstances of the system. IoT technology can also be utilized for communication between smart home appliances and a central controller. Researchers have proposed the IoT platform as a method of data gathering, monitoring, and control for the micro-grid. All devices and energy sources were merged and connected via this platform. Figure 10 illustrates the layers of the cloud platform, data processing layer, network layer, IoT platform layer, and agent layer.

It is challenging to develop a distributed Internet of Energy (IoE) infrastructure for energy management. The platform's functions include integrating the micro-grid tools into the communications infrastructure and connecting to the IoE cloud for device tracking and management. As shown in Figure 10, the proposed IoE communications network is composed of four separate levels. The descriptions of each stratum are provided below.

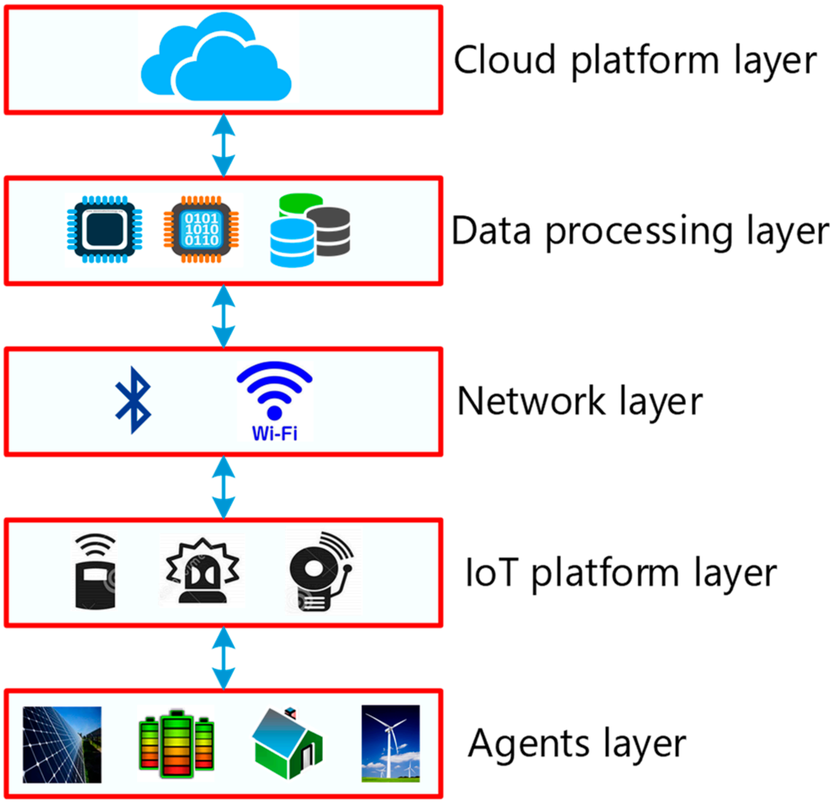

Figure 10. Suggested construction.

(a) Agent layer:

The device or perception layer is referred to as the layer of different components [45]. Various IoT users are included in the device layer, which comprises of smart electric vehicles, smart homes, and transportation systems, along with DGs like PVs and the WTs. Additionally, this layer supported different kinds of sensors for measuring the real-time environmental and physical state of the components and the actuators needed for adjusting them. Hence, WSNs and WSANs were seen to be inseparable components of this layer. The WSNs are defined as sensors which sense the environmental data and transmit it to other smart devices or the upper layers through the wireless network.

(b) IoT platform layer:

The IoT platform layer is the sensors layer. Additionally, this layer supports a number of sensors that may be used to monitor the connected agents' physical and environmental health and adjust in real time. The wireless sensor network and the wireless sensor and actor network (WSAN) are two components of the sheet that cannot be separated (WSNs). A WSN is a group of sensors that monitors the environment and broadcasts its findings to other devices or higher layers over a wireless network.

(c) Network layer:

The network layer has the ability to aggregate data from the cloud and perception layers before sending it to the upper layers for extra processing and storage. It can send data to other smart devices for distributed functionality that exists at component edges. A few examples of communication technologies that are used in a variety of settings are WiFi, Bluetooth, 3G/4G, Z-Wave, Zigbee, UMB, LoRa, and cellular networks. These devices are capable of wireless communication and have a wide range of uses.

(d) Data processing layer:

The data processing layer enables the storage and processing of a sizable amount of data that is gathered from lower levels with the aid of potent processors.

(e) Cloud layer:

For worldwide tracking, the cloud layer preserves past data from distributed energy resources. The ability to save historical data is one of the requirements for Internet of Everything apps and services [46]. Virtualized servers are a component of the IoE cloud layer. In addition, a new application interface with historical data preserved for each DER has been introduced. Application interface to the cloud infrastructure supports the historical archive, which may save and maintain a large amount of data [47].

The hierarchic structure for smart homes with physical layer, cyber layer, and control layer is presented in Figure 11. The hybrid platform features two communication layers. The Layer 1 devices in the intelligent building are found to transmit the MQTT messages to a built-in MQTT client (BMC), record the events/measures, and sign up for BMC's protection/control messages for MQTT. The interaction between the cloud and the BMC are defined in Layer 2 (global layer) using HTTP POST/GET requests. In this system, every computer has a Wi-Fi module connected to a local portal. This makes it possible to regularly write down the values of a particular and predetermined subject. Subscribing to the various topics, the BMC posts values to the cloud channel. The planned algorithm for system resource allocation is implemented by the cloud interface MATLAB, which has access to all cloud data. Then, the algorithm's output is sent from a cloud to smart BMC appliances that keep track of it. The researchers found that the suggested design was durable in the event of any layer's communication failing (either global or local). Therefore, the BMC was built in such a way that it could serve as a local controller (or backup controller) for all devices in the home in the event of a communication connection breakdown or significant latency seen in the network. The results section highlights this BMC feature [48–53].

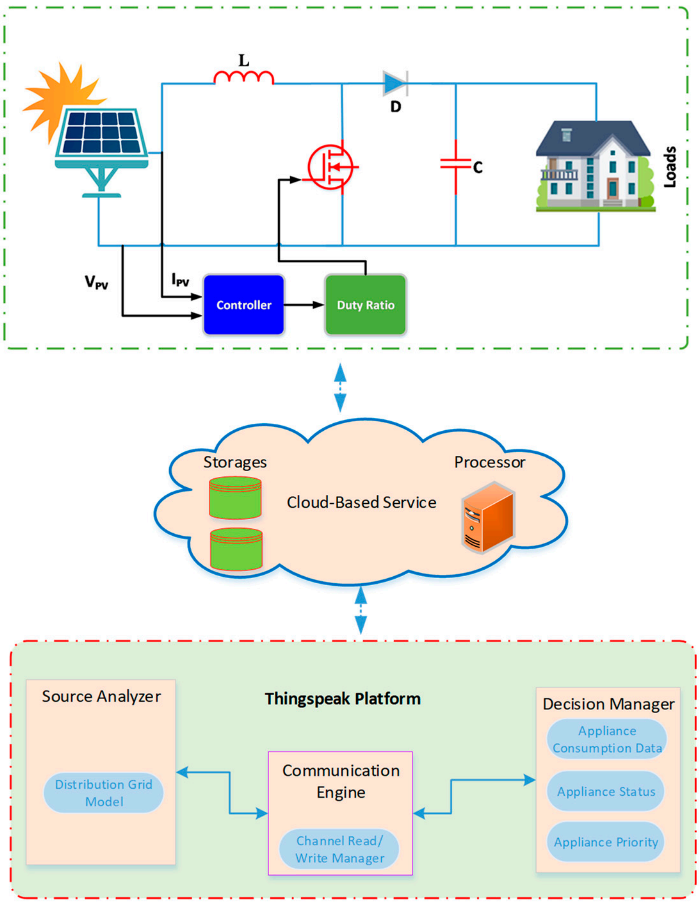

Figure 11. Proposed smart home architecture of communication.

7. Simulations Results

The results of the proposed method for addressing the issue of the examined microgrid system's optimal MPPT are described in this section; where the purpose was to achieve the MPPT of PV system. Moreover, a small-scale prototype, shown in Figure 1, was used to compare the performance of the proposed method with other state-of-the-art methods.

In this study, a Thing Speak platform was organized by a microcontroller, which served as the main command and control unit. Between SCADA and microgrid devices, MQTT served as a broker. Homeowners could interact with and acquire home energy management as a service via a cloud system, thanks to the simple and useful User Interface (UI) for the ThingSpeak platform created in this study. Figure 12 shows Supervisory Control and Data Acquisition (SCADA) architecture, Figure 12a shows the dashboard after the enter username and password, Figure 12b shows the user interface design platform.

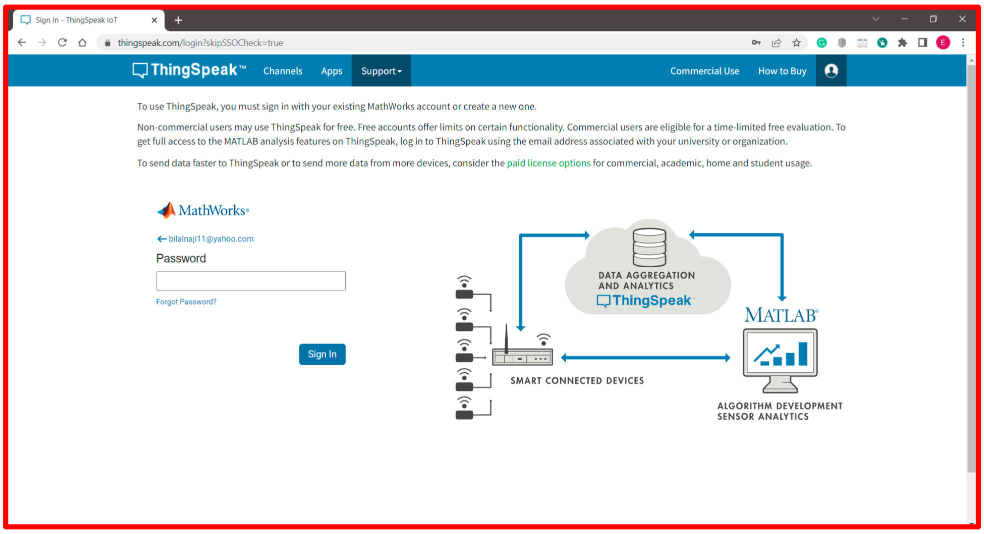

(a)

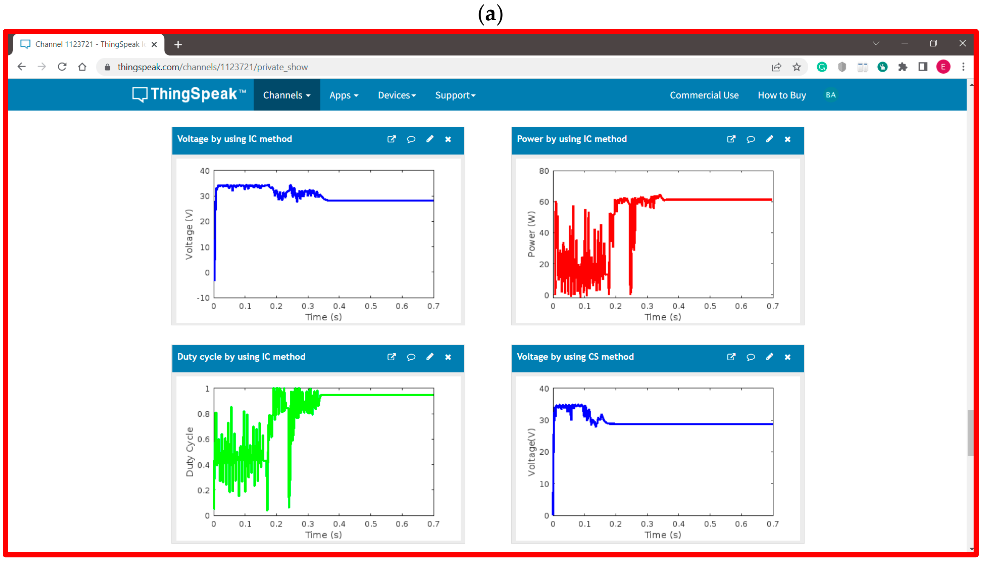

(b)

Figure 12. Supervisory Control and Data Acquisition (SCADA), (**a**) dashboard after the enter username and password, (**b**) user interface design platform.

A graphical user interface (GUI) was part of the suggested system to help users comprehend the overall voltage and power used. Figure 13 represents power consumption, voltage, and the duty cycle using the incremental conductance method as shown in [39]. Figure 14 shows the SCADA graphical user interface, (a) the voltage, (b) the power, and

(c) the duty cycle using the incremental conductance method. Figure 15 shows the power consumption, voltage, and duty cycle using the cuckoo search method. Figure 16 shows the SCADA graphical user interface, (a) the voltage, (b) the power, and (c) the duty cycle using the cuckoo search method. Figure 17 shows the power consumption, voltage, and duty cycle using the IABC method. Figure 18 shows the SCADA graphical user interface, (a) the voltage, (b) the power, and (c) the duty cycle using the IABC method.

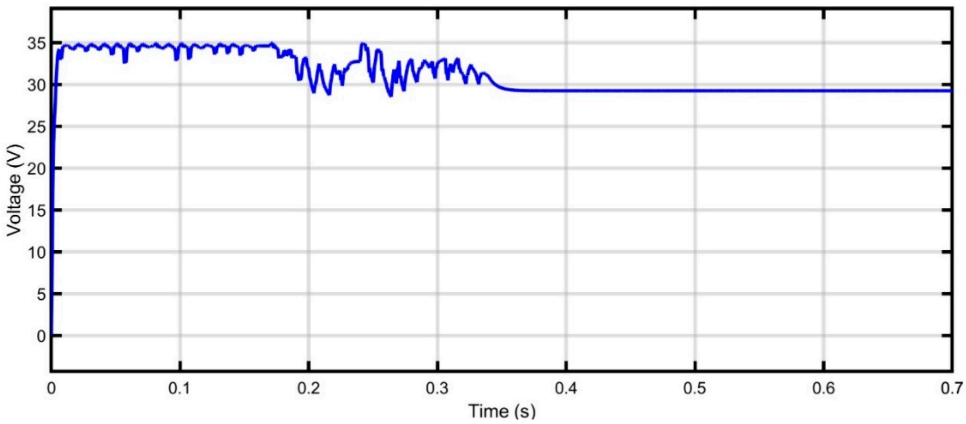

(**a**)

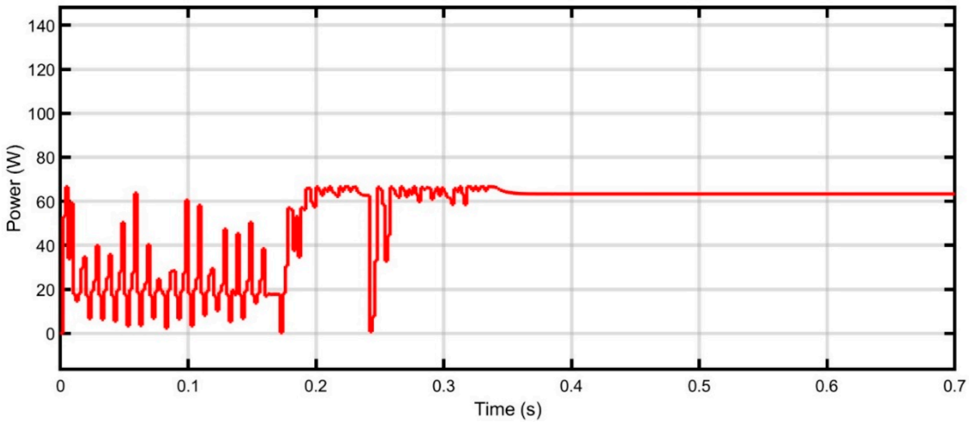

(**b**)

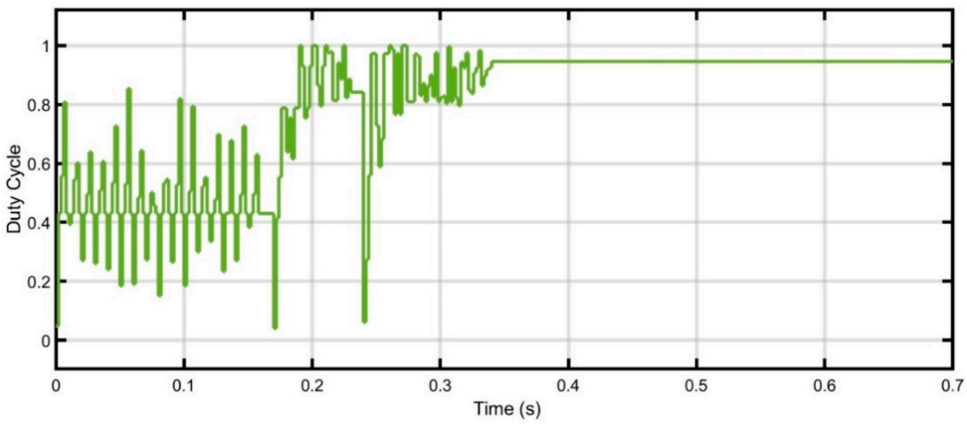

(**c**)

Figure 13. (**a**) The voltage, (**b**) the power, and (**c**) the duty cycle using the incremental conductance method.

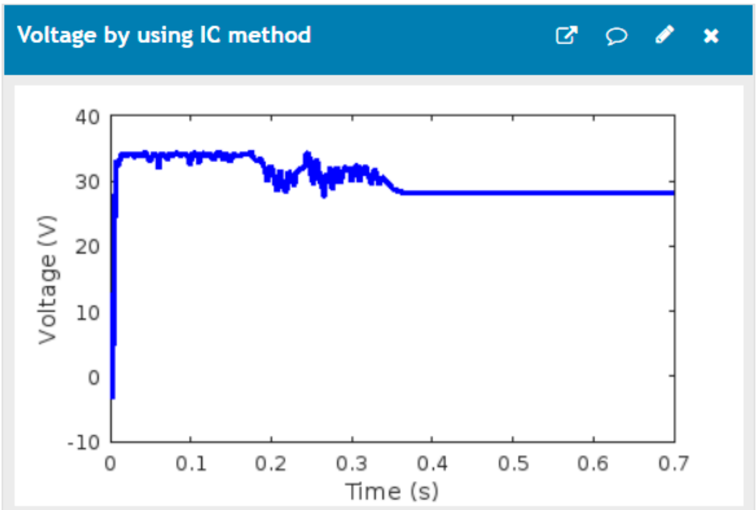

(**a**)

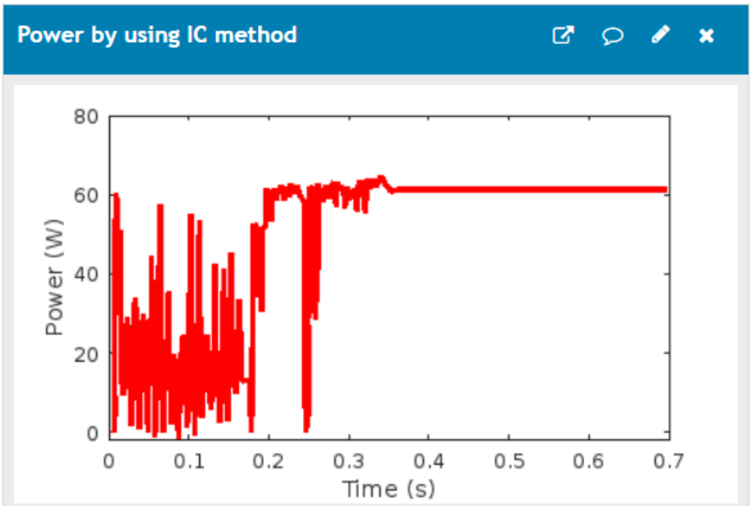

(**b**)

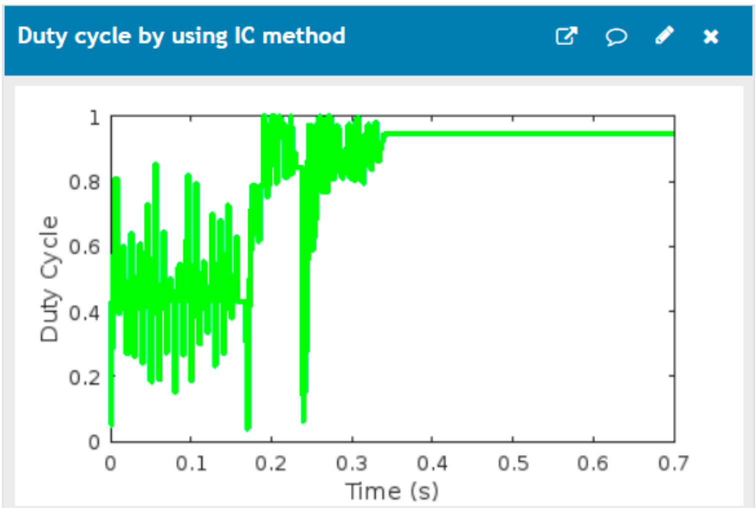

(**c**)

Figure 14. SCADA graphical user interface; (**a**) the voltage, (**b**) the power, and (**c**) the duty cycle using the incremental conductance method.

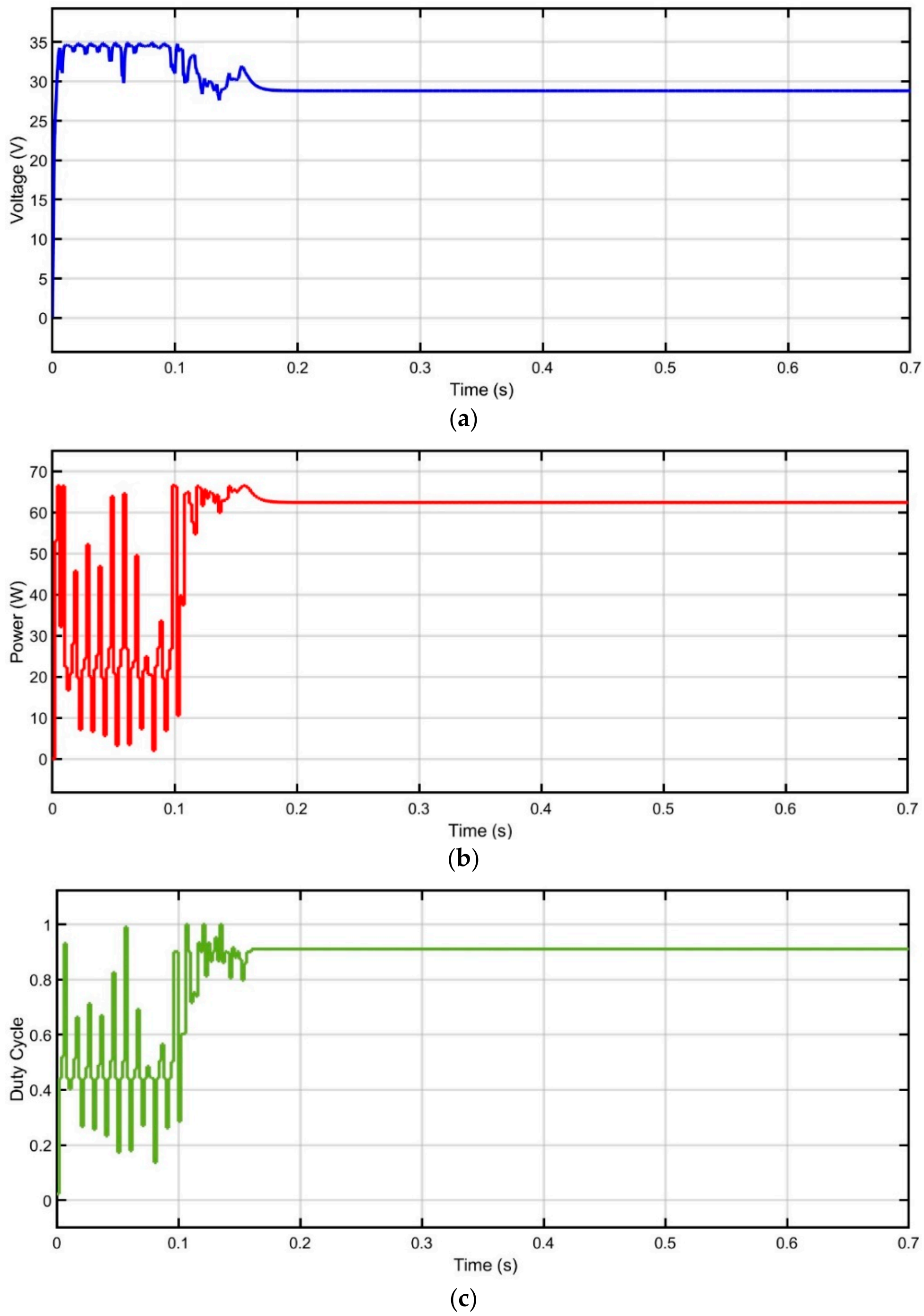

Figure 15. (**a**) The voltage, (**b**) the power, and (**c**) the duty cycle using the cuckoo search method.

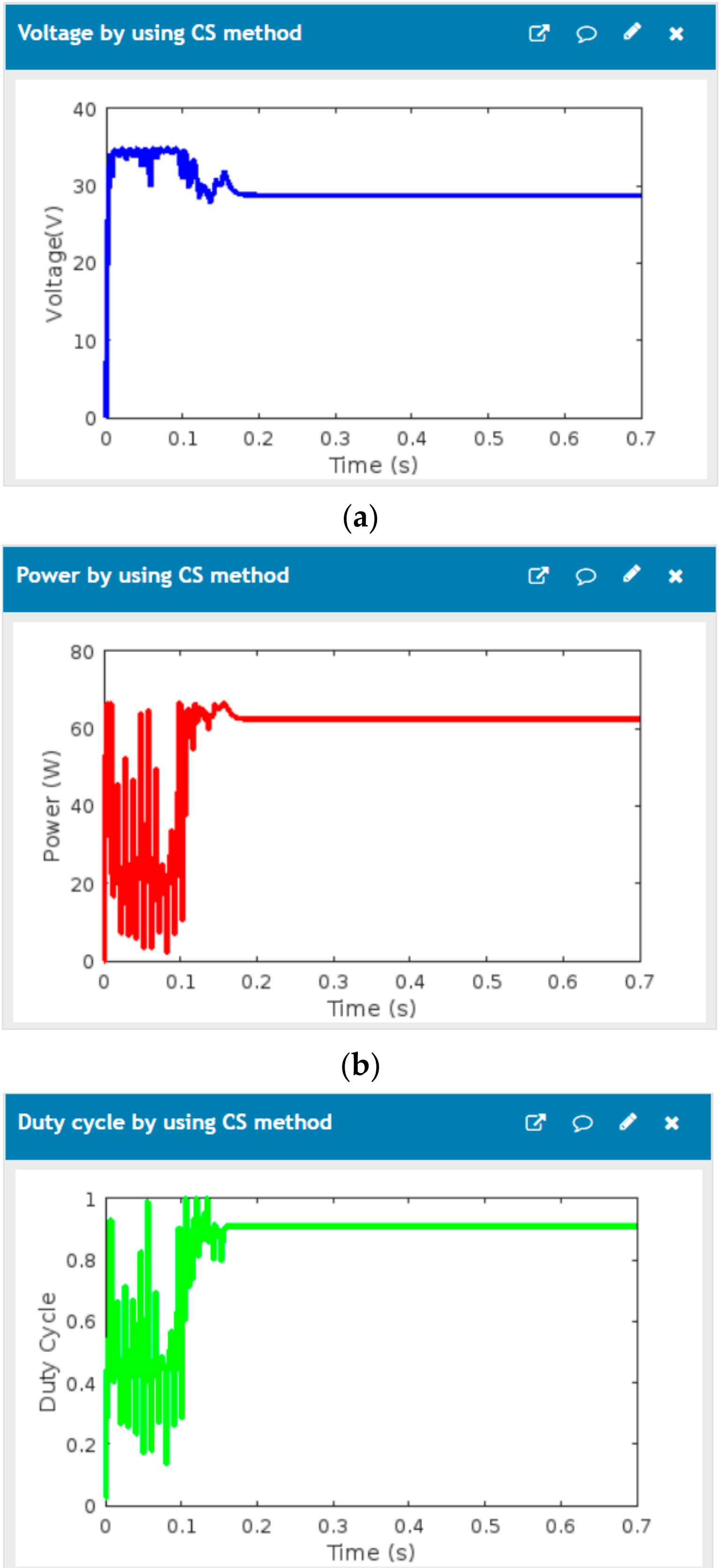

(**a**)

(**b**)

(**c**)

Figure 16. SCADA graphical user interface; (**a**) the voltage, (**b**) the power, and (**c**) the duty cycle using the cuckoo search method.

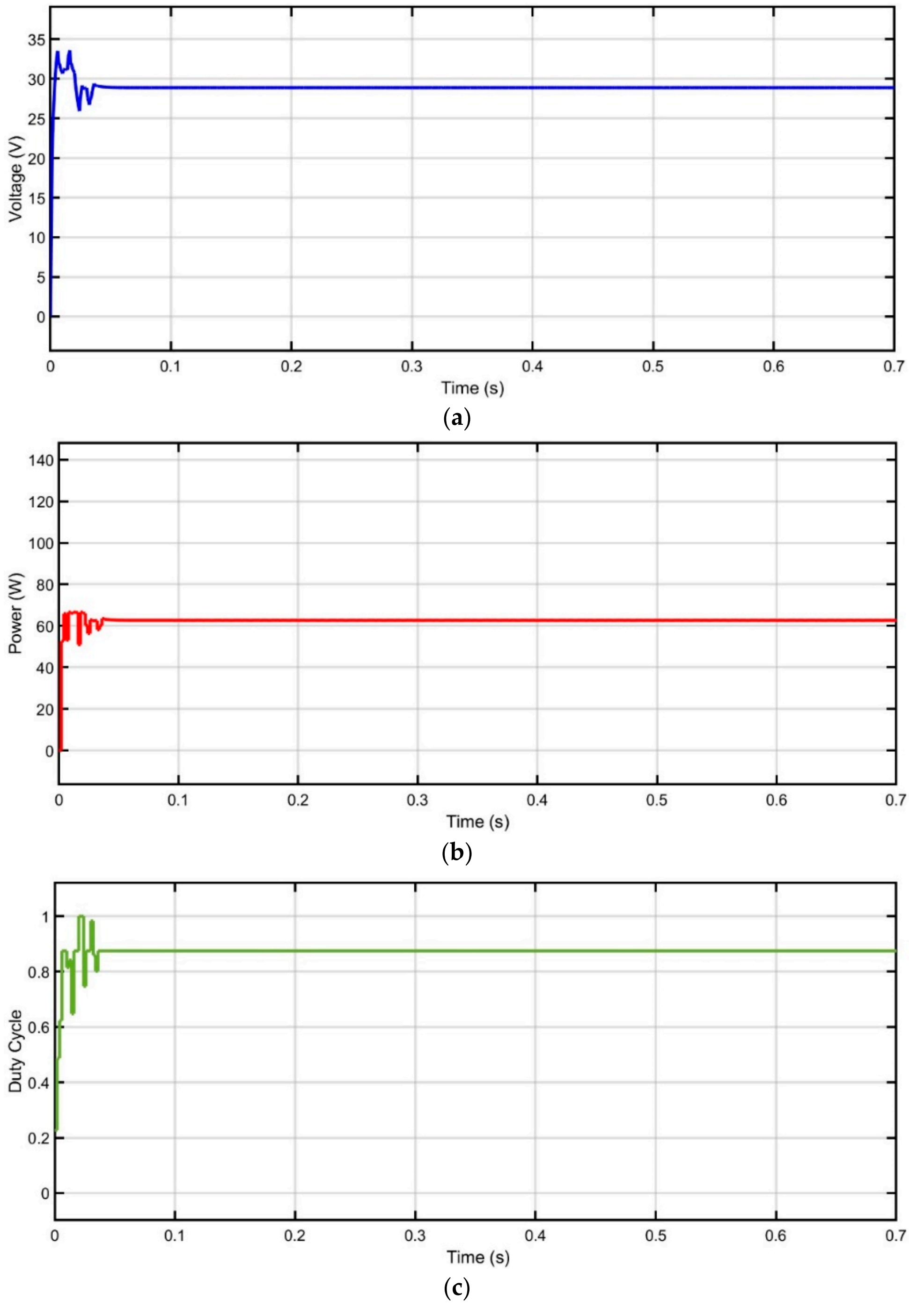

Figure 17. (**a**) The voltage, (**b**) the power, and (**c**) the duty cycle using the IABC method.

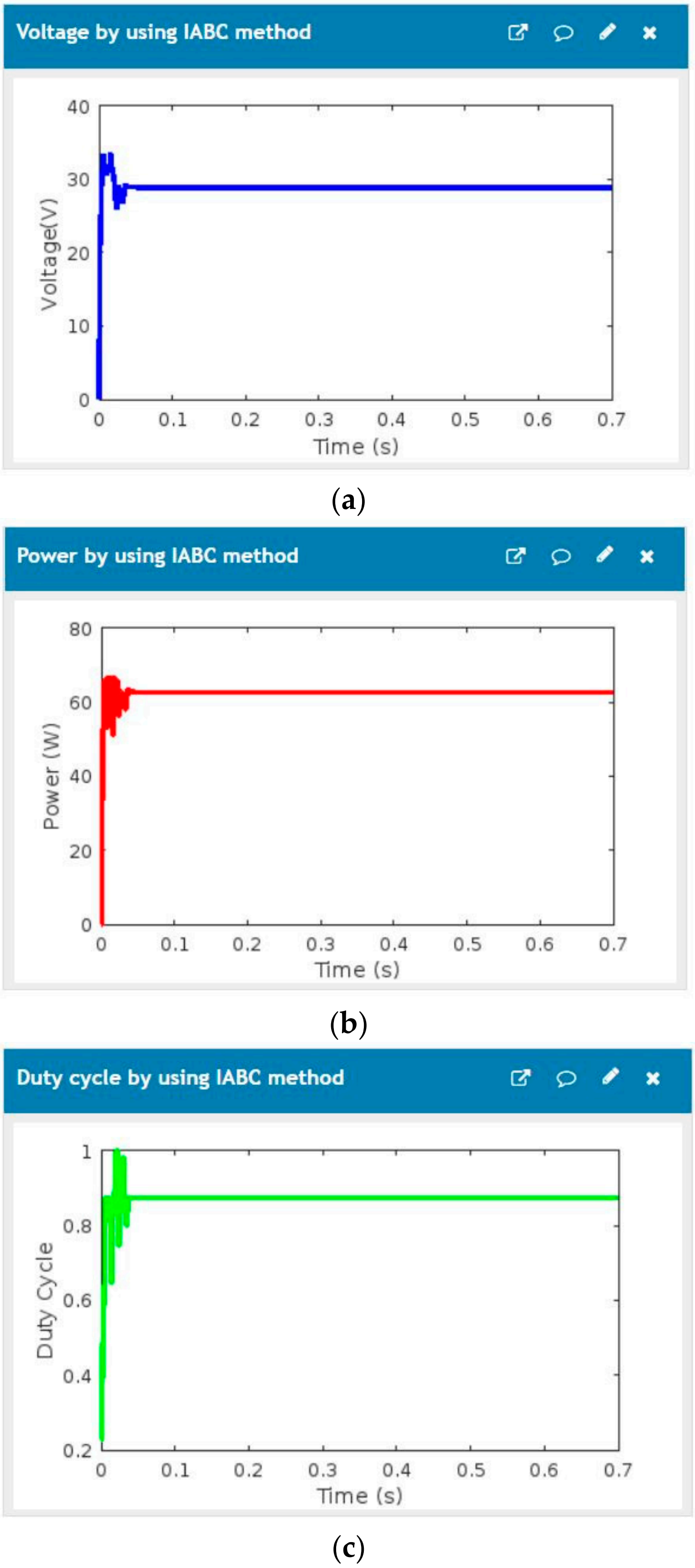

Figure 18. SCADA graphical user interface; (**a**) the voltage, (**b**) the power, and (**c**) the duty cycle using the IABC method.

8. Discussion of Results

The aforementioned Figures show the results of several algorithm simulations of photovoltaic power, photovoltaic voltage, and duty cycle.

Table 2 shows comparisons between the incremental conductance, cuckoo search, and improved artificial bee colony in terms of their steady-state restoration time, power, voltage, and the duty cycle. Figure 19 shows the steady-state restoration time using the incremental conductance method. Figure 20 shows the steady-state restoration time using the cuckoo search method. Figure 21 shows the steady-state restoration time using the improved artificial bee colony method.

Table 2. Comparison between the incremental conductance method, the cuckoo search method, and the improved artificial bee colony method.

Steady-State Restoration Time	Power (w)	Voltage (V)	Duty Cycle
Steady-state restoration time using IC method	0.355 (s)	0.357 (s)	0.356 (s)
Steady-state restoration time using cuckoo search method	0.18 (s)	0.182 (s)	0.185 (s)
Steady-state restoration time using IABC method	0.03 (s)	0.0298 (s)	0.0296 (s)

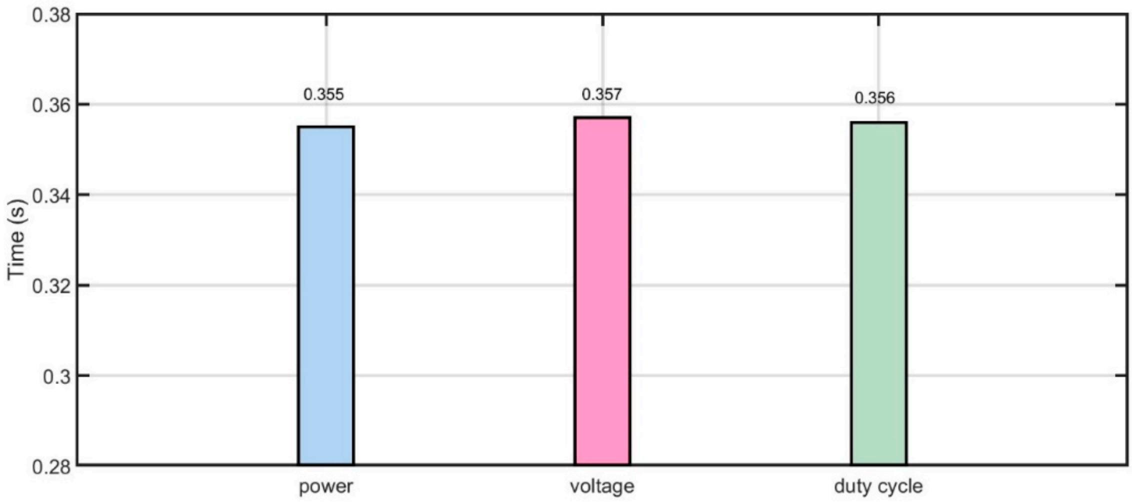

Figure 19. The steady-state restoration time using the incremental conductance method.

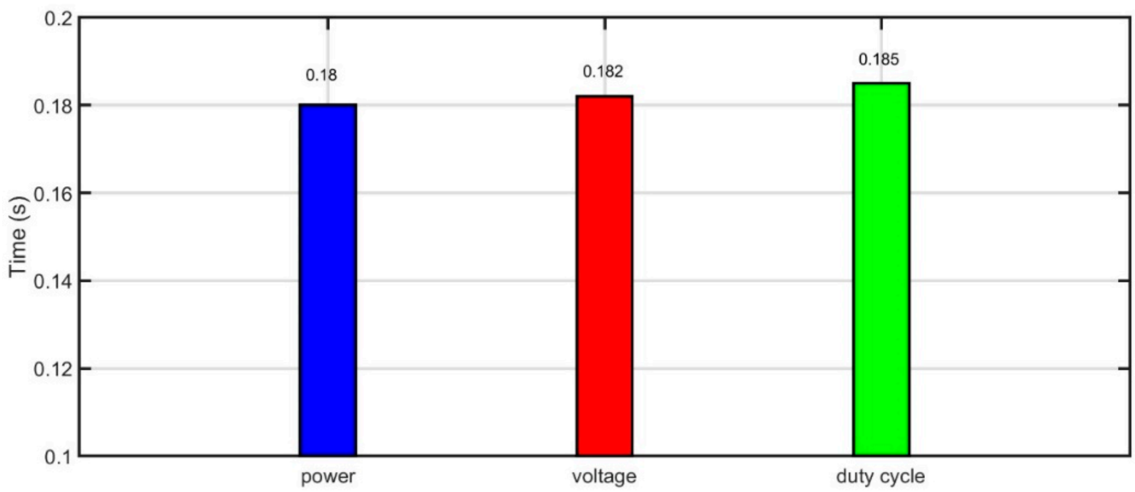

Figure 20. The steady-state restoration time using the cuckoo search method.

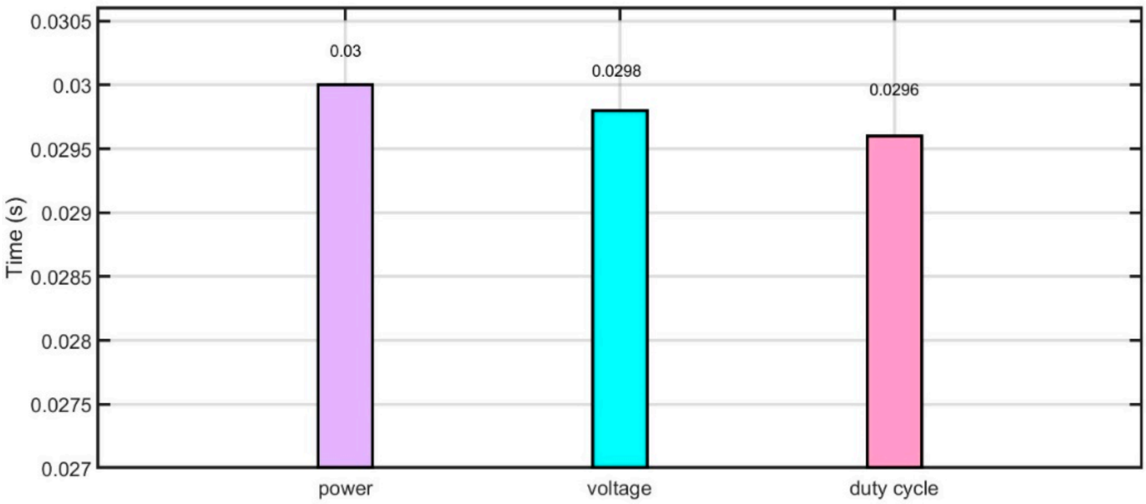

Figure 21. The steady-state restoration time using the IABC method.

The average efficiency and tracking time for the IABC approach were both 88% on average, which resulted in a faster time to MPPT. In addition, the tracking time of IABC method is reduced as compared to the algorithm in reference [39]. The results show that, thanks to reduced duty cycle randomness brought about by iterations, the suggested method outperforms the standard algorithm in terms of power fluctuations during the tracking period.

Figure 20 shows steady-state restoration time using the cuckoo search method. The tracking times are 0.18 s, 0.182 s, and 0.185 s, for the voltage, power, and duty cycle, respectively. The cuckoo search method achieved an efficiency of 80%, 78%, and 77%, respectively.

Figure 21 shows the steady-state restoration time using the IABC method. The tracking times are 0.03 s, 0.0298 s, and 0.0296 s, for the voltage, power, and duty cycle, respectively. The IABC method achieved an efficiency of 89%, 87%, and 88%, respectively. The incremental conductance method presented only large power fluctuations, but the IABC method obtained a faster MPPT with higher efficiency.

Figure 22 compares the steady-state restoration time obtained using the IC approach with the cuckoo search method. The proposed method can be used to maintain system stability in a timely manner. The steady-state restoration time are improved by 80%, 78%, and 77%, for the system's power, voltage, and duty cycle, respectively.

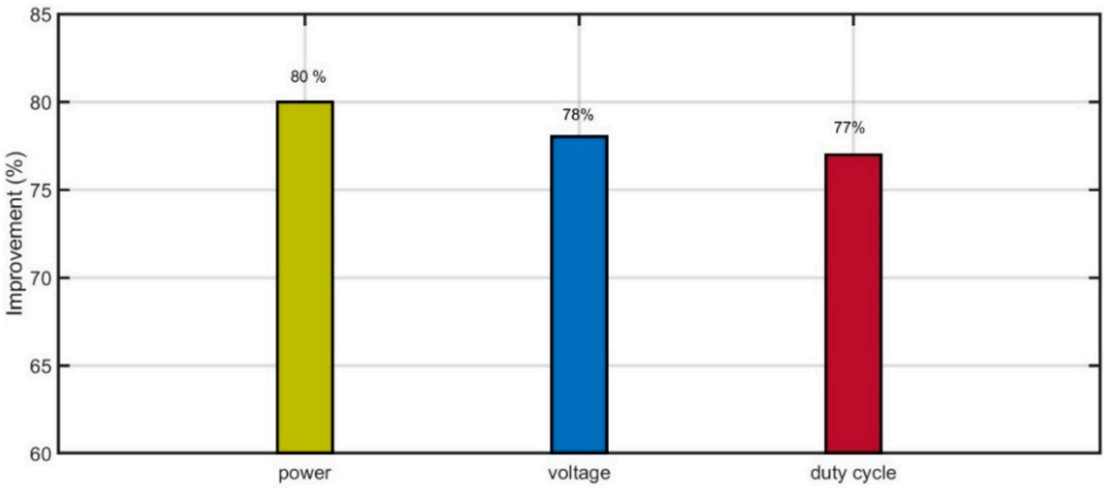

Figure 22. The comparison between the IC method and the cuckoo search method.

Figure 23 compares the steady-state restoration times obtained using the IC approach with the IABC method. The proposed method can be used to maintain system stability in a timely manner. The steady-state restoration time are improved by 89%, 87%, and 88% for the system's power, voltage, and duty cycle, respectively.

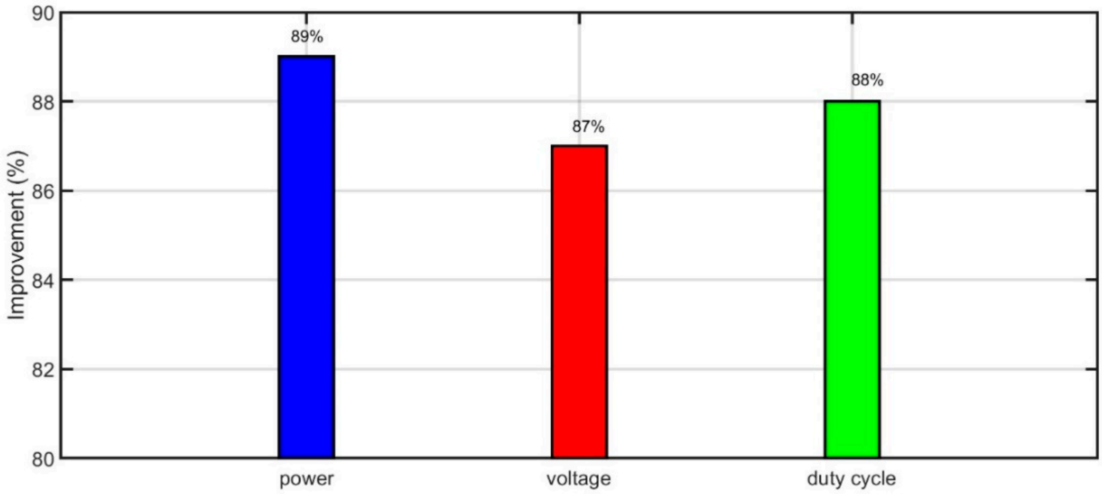

Figure 23. The comparison between the IC method and the IABC method.

From Figure 23, one can see that the IABC technique is more efficient than the incremental conductance and cuckoo search methods.

9. Conclusions

This paper investigated and outlined an issue in a traditional MPPT method, and presented a new approach to achieving MPPT for the photovoltaic systems using the IoT technique. As more and more renewable energy sources are included into the utility grid, using IoT to monitor a solar power plant is a crucial step. As a result, the monitoring of solar power plants will be automated and intellectualized, which will improve future grid integration and decision-making for large-scale solar power plants. This study presented IC, CS, and IABC-IoT-based MPPT trackers for photovoltaic power systems. The converter's duty ratio was adjusted to produce the most photovoltaic tracking power under fluctuating environmental conditions. Results demonstrated that the suggested control approach responds quickly and achieves steady-state operation more quickly than alternative control methods. After applying the cuckoo search method, the steady-state restoration times are improved by 80%, 78%, and 77% for the system's power, voltage, and duty cycle, respectively. Whereas, after applying the IABC method, the steady-state restoration times are improved by 89%, 87%, and 88% for the system's power, voltage, and duty cycle, respectively. Future work will aim to implement the proposed architecture in a laboratory environment, and compare the performance of the prototype with the simulation models.

Author Contributions: B.N.A.: writing—original draft, methodology, software, and validation; B.H.J.: supervisor, formal analysis, resources, investigation, editing, and writing—review; A.N.A.: formal analysis, writing, editing, and re-view; B.E.S.: review, and editing; A.M.J.: review, and editing; A.K.: review, and editing; V.B.: formal analysis; A.B. writing—review, P.S.: supervision, writing—review, and editing. All authors have read and agreed to the published version of the manuscript.

Funding: This research received no external funding.

Data Availability Statement: Not applicable.

Conflicts of Interest: The authors declare no conflict of interest.

Abbreviations

MPPT	Maximum Power Point Tracking
IoT	Internet of Things
IABC	Improved Artificial Bee Colony
PV	Photovoltaic
GMPP	Global Maximum Power Point
SCADA	Supervisory Control and Data Acquisition
V	Voltage
P	Power
WT	Wind Turbine
FC	Fuel Cell
SEPIC	Single-Ended Primary-Inductor Converter
IP	Internet Protocol
CS	Cuckoo Search
PSO	Particle Swarm Optimizer
PWM	Pulse Width Modulation
DERs	Distributed Energy Resources
BMC	Built-in MQTT Client
GUI	Graphical User Interface
IC	Incremental Conductance

References

1. Hafeez, M.A.; Naeem, A.; Akram, M.; Javed, M.Y.; Asghar, A.B.; Wang, Y. A Novel Hybrid MPPT Technique Based on Harris Hawk Optimization (HHO) and Perturb and Observer (P&O) under Partial and Complex Partial Shading Conditions. *Energies* **2022**, *15*, 5550. [CrossRef]
2. Manoharan, P.; Subramaniam, U.; Babu, T.S.; Padmanaban, S.; Holm-Nielsen, J.B.; Mitolo, M.; Ravichandran, S. Improved Perturb and Observation Maximum Power Point Tracking Technique for Solar Photovoltaic Power Generation Systems. *IEEE Syst. J.* **2021**, *15*, 3024–3035. [CrossRef]
3. Alhasnawi, B.N.; Jasim, B.H.; Sedhom, B.E.; Guerrero, J.M. Consensus Algorithm-based Coalition Game Theory for Demand Management Scheme in Smart Microgrid. *Sustain. Cities Soc.* **2021**, *74*, 103248. [CrossRef]
4. Alhasnawi, B.; Jasim, B.; Siano, P.; Guerrero, J. A Novel Real-Time Electricity Scheduling for Home Energy Management System Using the Internet of Energy. *Energies* **2021**, *14*, 3191. [CrossRef]
5. Alhasnawi, B.N.; Jasim, B.H. A new internet of things enabled trust distributed demand side management system. *Sustain. Energy Technol. Assessments* **2021**, *46*, 101272. [CrossRef]
6. Alhasnawi, B.; Jasim, B.; Rahman, Z.-A.; Siano, P. A Novel Robust Smart Energy Management and Demand Reduction for Smart Homes Based on Internet of Energy. *Sensors* **2021**, *21*, 4756. [CrossRef] [PubMed]
7. Alhasnawi, B.N.; Jasim, B.H. SCADA controlled smart home using Raspberry Pi3. In Proceedings of the 2018 International Conference on Advance of Sustainable Engineering and Its Ap-plication (ICASEA), Wasit-Kut, Iraq, 14–15 March 2018. [CrossRef]
8. Priyadarshi, N.; Padmanaban, S.; Holm-Nielsen, J.B.; Bhaskar, M.S.; Azam, F. Internet of things augmented a novel PSO-employed modified zeta converter-based photovoltaic maximum power tracking system: Hardware realisation. *IET Power Electron.* **2020**, *13*, 2775–2781. [CrossRef]
9. Adhya, S.; Saha, D.; Das, A.; Jana, J.; Saha, H. An IoT based smart solar photovoltaic remote monitoring and control unit. In Proceedings of the 2016 2nd International Conference on Control, Instrumentation, Energy & Communication (CIEC), Kolkata, India, 28–30 January 2016.
10. Khan, M.J.; Kumar, D.; Narayan, Y.; Malik, H.; Márquez, F.P.G.; Muñoz, C.Q.G. A Novel Artificial Intelligence Maximum Power Point Tracking Technique for Integrated PV-WT-FC Frameworks. *Energies* **2022**, *15*, 3352. [CrossRef]
11. Rouibah, N.; Barazane, L.; Benghanem, M.; Mellit, A. IoT-based low-cost prototype for online monitoring of maximum output power of domestic photovoltaic systems. *ETRI J.* **2021**, *43*, 459–470. [CrossRef]
12. Fathy, A.; Ben Atitallah, A.; Yousri, D.; Rezk, H.; Al-Dhaifallah, M. A new implementation of the MPPT based raspberry Pi embedded board for partially shaded photovoltaic system. *Energy Rep.* **2022**, *8*, 5603–5619. [CrossRef]
13. Khaleel, K.; Atyia, T.H.; Al-Naib, A.M.I. Design and Development of Re-al-Time Data Acquisition of Photovoltaic Panel Parameters via IoT. *NTU J. Renew. Energy* **2022**, *3*, 1–8.
14. Rani, D.P.; Suresh, D.; Kapula, P.R.; Akram, C.M.; Hemalatha, N.; Soni, P.K. IoT based smart solar energy monitoring systems. *Mater. Today Proc.* **2021**. [CrossRef]
15. Malar, A.J.G.; Kumar, C.A.; Saravanan, A.G. Iot based sustainable wind green energy for smart cites using fuzzy logic based fractional order darwinian particle swarm optimization. *Measurement* **2020**, *166*, 108208. [CrossRef]

16. Zafar, M.H.; Khan, N.M.; Mirza, A.F.; Mansoor, M.; Akhtar, N.; Qadir, M.U.; Khan, N.A.; Moosavi, S.K.R. A novel meta-heuristic optimization algorithm based MPPT control technique for PV systems under complex partial shading condition. *Sustain. Energy Technol. Assess.* **2021**, *47*, 101367. [CrossRef]
17. Shams, I.; Mekhilef, S.; Tey, K.S. Maximum Power Point Tracking Using Modified Butterfly Optimization Algorithm for Partial Shading, Uniform Shading, and Fast Varying Load Conditions. *IEEE Trans. Power Electron.* **2021**, *36*, 5569–5581. [CrossRef]
18. Nagadurga, T.; Narasimham, P.V.R.L.; Vakula, V.S.; Devarapalli, R.; Márquez, F.P.G. Enhancing Global Maximum Power Point of Solar Photovoltaic Strings under Partial Shading Conditions Using Chimp Optimization Algorithm. *Energies* **2021**, *14*, 4086. [CrossRef]
19. Fares, D.; Fathi, M.; Shams, I.; Mekhilef, S. A novel global MPPT technique based on squirrel search algorithm for PV module under partial shading conditions. *Energy Convers. Manag.* **2021**, *230*, 113773. [CrossRef]
20. Barbosa, E.J.; Cavalcanti, M.C.; Azevedo, G.M.D.S.; Bradaschia, F.; Limongi, L.R. Global Hybrid Maximum Power Point Tracking for PV Modules Based on a Double-Diode Model. *IEEE Access* **2021**, *9*, 158440–158455. [CrossRef]
21. Chao, K.-H.; Li, J.-Y. Global Maximum Power Point Tracking of Photovoltaic Module Arrays Based on Improved Artificial Bee Colony Algorithm. *Electronics* **2022**, *11*, 1572. [CrossRef]
22. Sayyad, J.; Nasikkar, P. Design and Development of Low Cost, Portable, On-Field I-V Curve Tracer Based on Capacitor Loading for High Power Rated Solar Photovoltaic Modules. *IEEE Access* **2021**, *9*, 70715–70731. [CrossRef]
23. Kumar, V.; Mitra, A.; Shaklya, O.; Sharma, S.; Rana, K. An adaptive robust fuzzy PI controller for maximum power point tracking of photovoltaic system. *Optik* **2022**, *259*, 168942. [CrossRef]
24. Dileep, G.; Singh, S. An improved particle swarm optimization based maximum power point tracking algorithm for PV system operating under partial shading conditions. *Sol. Energy* **2017**, *158*, 1006–1015. [CrossRef]
25. Liu, Y.-H.; Huang, S.-C.; Huang, J.-W.; Liang, W.-C. A Particle Swarm Optimization-Based Maximum Power Point Tracking Algorithm for PV Systems Operating Under Partially Shaded Conditions. *IEEE Trans. Energy Convers.* **2012**, *27*, 1027–1035. [CrossRef]
26. Rajasekar, N.; Vysakh, M.; Thakur, H.V.; Azharuddin, S.M.; Muralidhar, K.; Paul, D.; Jacob, B.; Balasubramanian, K.; Babu, T.S. Application of Modified Particle Swarm Optimization for Maximum Power Point Tracking under Partial Shading Condition. *Energy Procedia* **2014**, *61*, 2633–2639. [CrossRef]
27. Mirhassani, S.M.; Golroodbari, S.Z.M.; Mekhilef, S. An improved particle swarm optimization based maximum power point tracking strategy with variable sampling time. *Int. J. Electr. Power Energy Syst.* **2015**, *64*, 761–770. [CrossRef]
28. Tan, R.H.G.; Tinakaran, G.K. Development of battery energy storage system model in MATLAB/Simulink. *Int. J. Smart Grid Clean Energy* **2020**, *9*, 180–188. [CrossRef]
29. Tan, R.H.; Er, C.K.; Solanki, S.G. Modeling of Photovoltaic MPPT Lead Acid Battery Charge Controller for Standalone System Applications. *E3S Web Conf.* **2020**, *182*, 03005. [CrossRef]
30. Alhasnawi, B.N.; Jasim, B.H. A New Energy Management System of On-Grid/off-Grid Using Adaptive Neuro-Fuzzy Inference System. *J. Eng. Sci. Technol.* **2020**, *15*, 3903–3919.
31. Forcan, M.; Maksimović, M. Cloud-Fog-based approach for Smart Grid monitoring. *Simul. Model. Pract. Theory* **2020**, *101*, 101988. [CrossRef]
32. Ouramdane, O.; Elbouchikhi, E.; Amirat, Y.; Le Gall, F.; Gooya, E.S. Home Energy Management Considering Renewable Resources, Energy Storage, and an Electric Vehicle as a Backup. *Energies* **2022**, *15*, 2830. [CrossRef]
33. Alhasnawi, B.; Jasim, B. A New Coordinated Control of Hybrid Microgrids with Renewable Energy Resources Under Variable Loads and Generation Conditions. *Iraqi J. Electr. Electron. Eng.* **2020**, *16*, 1–20. [CrossRef]
34. Luna, A.C.; Diaz, N.L.; Graells, M.; Vasquez, J.C.; Guerrero, J.M. Mixed-Integer-Linear-Programming-Based Energy Management System for Hybrid PV-Wind-Battery Microgrids: Modeling, Design, and Experimental Verification. *IEEE Trans. Power Electron.* **2017**, *32*, 2769–2783. [CrossRef]
35. Alhasnawi, B.; Jasim, B. Adaptive Energy Management System for Smart Hybrid Microgrids. In Proceedings of the 3rd Scientific Conference of Electrical and Electronic Engineering Researches (SCEEER), Basrah, Iraq, 15–16 June 2020. [CrossRef]
36. Alhasnawi, B.N.; Jasim, B.H.; Issa, W.; Anvari-Moghaddam, A.; Blaabjerg, F. A New Robust Control Strategy for Parallel Operated Inverters in Green Energy Applications. *Energies* **2020**, *13*, 3480. [CrossRef]
37. Alhasnawi, B.N.; Jasim, B.H.; Esteban, M.D. A New Robust Energy Management and Control Strategy for a Hybrid Microgrid System Based on Green Energy. *Sustainability* **2020**, *12*, 5724. [CrossRef]
38. Alhasnawi, B.N.; Jasim, B.H.J. A Novel Hierarchical Energy Management System Based on Optimization for Multi-Microgrid. *Int. J. Electr. Eng. Inform.* **2020**, *12*, 586–606. [CrossRef]
39. Aldair, A.; Obed, A.; Halihal, A.F. Design and implementation of ANFIS-reference model controller based MPPT using FPGA for photovoltaic system. *Renew. Sustain. Energy Rev.* **2018**, *82*, 2202–2217. [CrossRef]
40. Halihal, A.F. Design and Implementation of Neuro-Fuzzy Controller Using FPGA for Sun Tracking System. Master's Thesis, the College of Engineering, University of Basrah, Basrah, Iraq, 2016; pp. 1–154.
41. Yang, X.-S.; Deb, S. Cuckoo Search via Lvy flights. In Proceedings of the 2009 World Congress Nature & Biologically Inspired Computing (NaBIC), Coimbatore, India, 9–11 December 2009; pp. 210–214. [CrossRef]
42. Bentata, K.; Mohammedi, A.; Benslimane, T. Development of rapid and relia-ble cuckoo search algorithm for global maximum power point tracking of solar PV systems in partial shading condition. *Arch. Control. Sci.* **2021**, *31*, 495–526. [CrossRef]

43. Ahmed, J.; Salam, Z. A Maximum Power Point Tracking (MPPT) for PV system using Cuckoo Search with partial shading capability. *Appl. Energy* **2014**, *119*, 118–130. [CrossRef]
44. Sundareswaran, K.; Sankar, P.; Nayak, P.S.R.; Simon, S.P.; Palani, S. Enhanced Energy Output from a PV System Under Partial Shaded Conditions Through Artificial Bee Colony. *IEEE Trans. Sustain. Energy* **2015**, *6*, 198–209. [CrossRef]
45. Tajalli, S.Z.; Mardaneh, M.; Taherian-Fard, E.; Izadian, A.; Kavousi-Fard, A.; Dabbaghjamanesh, M.; Niknam, T. DoS-Resilient Distributed Optimal Sched-uling in a Fog Supporting IIoT-Based Smart Microgrid. *IEEE Trans. Ind. Appl.* **2020**, *56*, 2968–2977. [CrossRef]
46. Alhasnawi, B.N.; Jasim, B.H. Internet of Things (IoT) for smart grids: A comprehensive review. *J. Xi'an Univ. Arch.* **2020**, *63*, 1006–7930.
47. Marzal, S.; González-Medina, R.; Salas-Puente, R.; Garcerá, G.; Figueres, E. An Em-bedded Internet of Energy Communication Platform for the Future Smart Microgrids Management. *IEEE Internet Things J.* **2019**, *6*, 7241–7252. [CrossRef]
48. Alhasnawi, B.; Jasim, B.; Rahman, Z.-A.; Guerrero, J.; Esteban, M. A Novel Internet of Energy Based Optimal Multi-Agent Control Scheme for Microgrid including Renewable Energy Resources. *Int. J. Environ. Res. Public Health* **2021**, *18*, 8146. [CrossRef] [PubMed]
49. Alhasnawi, B.; Jasim, B.; Sedhom, B.; Hossain, E.; Guerrero, J. A New Decentralized Control Strategy of Microgrids in the Internet of Energy Paradigm. *Energies* **2021**, *14*, 2183. [CrossRef]
50. Bahmanyar, D.; Razmjooy, N.; Mirjalili, S. Multi-objective scheduling of IoT-enabled smart homes for energy management based on Arithmetic Optimization Algorithm: A Node-RED and Node MCU module-based technique. *Knowl. Based Syst.* **2022**, *247*, 108762. [CrossRef]
51. Alhasnawi, B.N.; Jasim, B.H.; Mansoor, R.; Alhasnawi, A.N.; A Rahman, Z.S.; Alhelou, H.H.; Guerrero, J.M.; Dakhil, A.M.; Siano, P. A new Internet of Things based optimization scheme of residential demand side management system. *IET Renew. Power Gener.* **2022**, *16*, 1992–2006. [CrossRef]
52. Alhasnawi, B.N.; Jasim, B.H.; Siano, P.; Alhelou, H.H.; Al-Hinai, A. A Novel Solution for Day-Ahead Scheduling Problems Using the IoT-Based Bald Eagle Search Optimization Algorithm. *Inventions* **2022**, *7*, 48. [CrossRef]
53. Alhasnawi, B.; Jasim, B.; Esteban, M.; Guerrero, J. A Novel Smart Energy Management as a Service over a Cloud Computing Platform for Nanogrid Appliances. *Sustainability* **2020**, *12*, 9686. [CrossRef]